26. Sumpter R, Jr., Loo YM, Foy E, Li K, Yoneyama M, et al. (2005) Regulating intracellular antiviral defense and permissiveness to hepatitis C virus RNA replication through a cellular RNA helicase, RIG-I. J Virol 79: 2689–2699.
27. Yi M, Lemon SM (2004) Adaptive mutations producing efficient replication of genotype 1a hepatitis C virus RNA in normal Huh7 cells. J Virol 78: 7904–7915.
28. Li K, Li NL, Wei D, Pfeffer SR, Fan M, et al. (2012) Activation of chemokine and inflammatory cytokine response in hepatitis C virus-infected hepatocytes depends on Toll-like receptor 3 sensing of hepatitis C virus double-stranded RNA intermediates. Hepatology 55: 666–675.
29. Tuplin A, Evans DJ, Simmonds P (2004) Detailed mapping of RNA secondary structures in core and NS5B-encoding region sequences of hepatitis C virus by RNase cleavage and novel bioinformatic prediction methods. J GenVirol 85: 3037–3047.
30. Kato N, Ikeda M, Mizutani T, Sugiyama K, Noguchi M, et al. (1996) Replication of hepatitis C virus in cultured non-neoplastic human hepatocytes. Japanese Journal of Cancer Research (Amsterdam) 87: 787–792.
31. Leonard JN, Ghirlando R, Askins J, Bell JK, Margulies DH, et al. (2008) The TLR3 signaling complex forms by cooperative receptor dimerization. Proc Natl Acad Sci U S A 105: 258–263.
32. Kodama T, Freeman M, Rohrer L, Zabrecky J, Matsudaira P, et al. (1990) Type I macrophage scavenger receptor contains alpha-helical and collagen-like coiled coils. Nature 343: 531–535.
33. Shimakami T, Yamane D, Jangra RK, Kempf BJ, Spaniel C, et al. (2012) Stabilization of hepatitis C RNA by an Ago2-miR-122 complex. Proc Natl Acad Sci U S A 109: 941–946.
34. Anachi RB, Siegel DL, Baum J, Brodsky B (1995) Acid destabilization of a triple-helical peptide model of the macrophage scavenger receptor. FEBS Lett 368: 551–555.
35. Ma Y, Anantpadma M, Timpe JM, Shanmugam S, Singh SM, et al. (2011) Hepatitis C virus NS2 protein serves as a scaffold for virus assembly by interacting with both structural and nonstructural proteins. J Virol 85: 86–97.
36. Li Y, Masaki T, Yamane D, McGivern DR, Lemon SM (2013) Competing and noncompeting activities of miR-122 and the 5′ exonuclease Xrn1 in regulation of hepatitis C virus replication. Proc Natl Acad Sci U S A 110: 1881–1886.
37. Kannan RP, Hensley LL, Evers L, Lemon SM, McGivern DR (2011) Hepatitis C virus infection causes cell cycle arrest at the level of entry to mitosis. J Virol 85: 7989–8001.
38. Suzuki H, Kurihara Y, Takeya M, Kamada N, Kataoka M, et al. (1997) A role for macrophage scavenger receptors in atherosclerosis and susceptibility to infection. Nature 386: 292–296.
39. Yew KH, Carsten B, Harrison C (2010) Scavenger receptor A1 is required for sensing HCMV by endosomal TLR-3/-9 in monocytic THP-1 cells. Mol Immunol 47: 883–893.
40. Freeman M, Ashkenas J, Rees DJ, Kingsley DM, Copeland NG, et al. (1990) An ancient, highly conserved family of cysteine-rich protein domains revealed by cloning type I and type II murine macrophage scavenger receptors. Proc Natl Acad Sci U S A 87: 8810–8814.
41. Doi T, Higashino K, Kurihara Y, Wada Y, Miyazaki T, et al. (1993) Charged collagen structure mediates the recognition of negatively charged macromolecules by macrophage scavenger receptors. J Biol Chem 268: 2126–2133.
42. Doi T, Kurasawa M, Higashino K, Imanishi T, Mori T, et al. (1994) The histidine interruption of an alpha-helical coiled coil allosterically mediates a pH-dependent ligand dissociation from macrophage scavenger receptors. J Biol Chem 269: 25598–25604.
43. Takahashi K, Asabe S, Wieland S, Garaigorta U, Gastaminza P, et al. (2010) Plasmacytoid dendritic cells sense hepatitis C virus-infected cells, produce interferon, and inhibit infection. Proc Natl Acad Sci U S A 107: 7625–7626.
44. Blight KJ, McKeating JA, Rice CM (2002) Highly permissive cell lines for subgenomic and genomic hepatitis C virus RNA replication. J Virol 76: 13001–13014.
45. Ikeda M, Sugiyama K, Mizutani T, Tanaka T, Tanaka K, et al. (1998) Human hepatocyte clonal cell lines that support persistent replication of hepatitis C virus. Virus Res 56: 157–167.
46. Wakita T, Pietschmann T, Kato T, Date T, Miyamoto M, et al. (2005) Production of infectious hepatitis C virus in tissue culture from a cloned viral genome. Nature Medicine 11: 791–796.
47. Yi M, Ma Y, Yates J, Lemon SM (2007) Compensatory mutations in E1, p7, NS2, and NS3 enhance yields of cell culture-infectious intergenotypic chimeric hepatitis C virus. J Virol 81: 629–638.
48. Ma Y, Yates J, Liang Y, Lemon SM, Yi M (2008) NS3 helicase domains involved in infectious intracellular hepatitis C virus particle assembly. J Virol 82: 7624–7639.
49. Shimakami T, Yamane D, Welsch C, Hensley L, Jangra RK, et al. (2012) Base-pairing between Hepatitis C Virus RNA and miR-122 3′ of its Seed Sequence is Essential for Genome Stabilization and Production of Infectious Virus. J Virol 86(13): 7372–7383.
50. Lin R, Genin P, Mamane Y, Hiscott J (2000) Selective DNA binding and association with the CREB binding protein coactivator contribute to differential activation of alpha/beta interferon genes by interferon regulatory factors 3 and 7. Mol Cell Biol 20: 6342–6353.
51. Fredericksen B, Akkaraju GR, Foy E, Wang C, Pflugheber J, et al. (2002) Activation of the interferon-beta promoter during hepatitis C virus RNA replication. Viral Immunol 15: 29–40.
52. Akagi T, Sasai K, Hanafusa H (2003) Refractory nature of normal human diploid fibroblasts with respect to oncogene-mediated transformation. Proc Natl Acad Sci U S A 100: 13567–13572.
53. Dansako H, Naganuma A, Nakamura T, Ikeda F, Nozaki A, et al. (2003) Differential activation of interferon-inducible genes by hepatitis C virus core protein mediated by the interferon stimulated response element. Virus Res 97: 17–30.
54. Naganuma A, Dansako H, Nakamura T, Nozaki A, Kato N (2004) Promotion of microsatellite instability by hepatitis C virus core protein in human non-neoplastic hepatocyte cells. Cancer Res 64: 1307–1314.
55. Dansako H, Ikeda M, Ariumi Y, Wakita T, Kato N (2009) Double-stranded RNA-induced interferon-beta and inflammatory cytokine production modulated by hepatitis C virus serine proteases derived from patients with hepatic diseases. Arch Virol 154: 801–810.
56. Dansako H, Naka K, Ikeda M, Kato N (2005) Hepatitis C virus proteins exhibit conflicting effects on the interferon system in human hepatocyte cells. Biochem Biophys Res Commun 336: 458–468.
57. Dansako H, Ikeda M, Kato N (2007) Limited suppression of the interferon-beta production by hepatitis C virus serine protease in cultured human hepatocytes. Febs J 274: 4161–4176.
58. Marchler-Bauer A, Lu S, Anderson JB, Chitsaz F, Derbyshire MK, et al. (2011) CDD: a Conserved Domain Database for the functional annotation of proteins. Nucleic Acids Res 39: D225–229.

OPEN ACCESS Freely available online

PLOS | ONE

Critical Role of Interferon-α Constitutively Produced in Human Hepatocytes in Response to RNA Virus Infection

Yoji Tsugawa[1,2], Hiroki Kato[3], Takashi Fujita[3], Kunitada Shimotohno[4], Makoto Hijikata[1,2]*

1 Laboratory of Human Tumor Viruses, Institute for Virus Research, Kyoto University, Kyoto, Japan, **2** Laboratory of Viral Oncology, Graduate School of Biostudies, Kyoto University, Kyoto, Japan, **3** Laboratory of Molecular Genetics, Institute for Virus Research, Kyoto University, Kyoto, Japan, **4** The Research Center for Hepatitis and Immunology, National Center for Global Health and Medicine, Ichikawa, Japan

Abstract

Several viruses are known to infect human liver and cause the hepatitis, but the interferon (IFN) response, a first-line defense against viral infection, of virus-infected hepatocytes is not clearly defined yet. We investigated innate immune system against RNA viral infection in immortalized human hepatocytes (HuS-E/2 cells), as the cells showed similar early innate immune responses to primary human hepatocytes (PHH). The low-level constitutive expression of IFN-α1 gene, but not IFN-β and IFN-λ, was observed in both PHH and HuS-E/2 cells in the absence of viral infection, suggesting a particular subtype(s) of IFN-α is constitutively produced in human hepatocytes. To examine the functional role of such IFN-α in the antiviral response, the expression profiles of innate immune-related genes were studied in the cells with the treatment of neutralization against type I IFN receptor 2 (IFNAR2) or IFN-α itself to inhibit the constitutive IFN-α signaling before and after virus infection. As the results, a clear reduction of basal level expression of IFN-inducible genes was observed in uninfected cells. When the effect of the inhibition on the cells infected with hepatitis C virus (HCV) was examined, the significant decrease of IFN stimulated gene expression and the enhancement of initial HCV replication were observed, suggesting that the steady-state production of IFN-α plays a role in amplification of antiviral responses to control the spread of RNA viral infection in human hepatocytes.

Citation: Tsugawa Y, Kato H, Fujita T, Shimotohno K, Hijikata M (2014) Critical Role of Interferon-α Constitutively Produced in Human Hepatocytes in Response to RNA Virus Infection. PLoS ONE 9(2): e89869. doi:10.1371/journal.pone.0089869

Editor: Hak Hotta, Kobe University, Japan

Received September 25, 2013; **Accepted** January 24, 2014; **Published** February 26, 2014

Funding: This work was supported by grants-in-aid from the Ministry of Health, Labour and Welfare of Japan. The funders had no role in study design, data collection and analysis, decision to publish, or preparation of the manuscript.

Competing Interests: The authors have declared that no competing interests exist.

* E-mail: mhijikat@virus.kyoto-u.ac.jp

Introduction

It has been shown that the replication of RNA viruses, including Sendai virus (SeV), Vesicular stomatitis virus, Newcastle disease virus, Sindbis virus, and Hepatitis C virus (HCV) is suppressed by type I interferon (IFN) (IFN-α and IFN-β) produced rapidly from the cells after infection of viruses [1,2]. The cytosolic RNA helicases, including retinoic acid-inducible gene (RIG)-I, have been identified as receptors of pathogen-associated molecular patterns of RNA viruses [3]. After recognition of RNA virus infection by those receptors, signal cascades for induction of IFNs are stimulated and result in the activation of IFN regulatory factor (IRF)-3, and IRF-7 which are transcription factors for induction of type I IFN genes [3,4]. IRF-3 is constitutively produced in many cell types and tissues and phosphorylated after virus infection. Phosphorylated IRF-3 forms a dimer (either a homodimer or a heterodimer with IRF-7) and is translocated to the nucleus. Unlike IRF-3, IRF-7 is constitutively produced only in small amounts, if any, but the gene expression is strongly induced by type I IFN-mediated signaling in most cell types and tissues. The produced IFNs by the way described above then are secreted from the viral infected cells and bind to their receptors, which consist of IFN α/β receptor (IFNAR1 and 2), on the surface of IFN producing and/or neighboring cells and deliver the IFN signal to those cells. The primary role of type I IFN is to limit spread of a variety of pathogens via initiation of the innate immune responses through induction of the genes encoding cytokines and antiviral proteins during the first days of infection [5]. These proteins exhibit antiviral effects both directly by inhibiting viral replication and indirectly by stimulating the adaptive immune system.

On the other hand, constitutive production of type I IFN has been detected in several cells without pathogen stimulation albeit at low level. The constitutive IFN-β has been revealed to be important in maintaining immune homeostasis and essential for immune cell priming [6]. In addition, type I IFN is also known to correlate with multiple biological activities, including anti-proliferative, anti-tumor, pro-apoptotic, and immunomodulatory functions [6,7]. Previously it was reported that the IFN-α mRNA was expressed in the human normal liver [8]. However, what cell type in the human liver is responsible for the expression and what is the biological role have not been clear yet.

Our previous data showed that immortalized human hepatocytes, HuS-E/2 cells, support the whole life cycle of blood-borne HCV (HCVbb) [9]. The infection and proliferation of HCVbb in HuS-E/2 cells were enhanced by ectopic expression of a dominant-negative form of IRF-7, but not that of IRF-3, suggesting that IRF-7, rather than IRF-3, plays a primary role in regulation of HCV proliferation in these cells [10]. IRF-7 mRNA was detected in primary hepatocytes (PHH) and HuS-E/2 cells, but not HuH-7 cells, one of hepatocellular carcinoma derived cell lines, without virus infection [10]. However, the role of

the preexisting IRF-7 and molecular mechanism of its constitutive expression in hepatocytes remains unclear, because of limited knowledge of immediate innate immune response in human hepatocytes.

As the result of study on innate immunity of human hepatocytes, here we report that active IFN-α release occurs in human hepatocytes even in the absence of virus infection. We additionally show that the constitutive IFN-α plays a critical role in the early induction of IFN genes and some IFN stimulated genes (ISGs) through the increase in expression of genes related with induction of such genes, including IRF-7 gene, before virus infection.

Materials and Methods

Cell Culture

HuH-7, Huh-7.5, HepG2, and 293FT cells were grown in Dulbecco's modified Eagle's medium (Nacalai Tesque, Kyoto, Japan) supplemented with 10% fetal bovine serum, 100 U/ml nonessential amino acids (Nacalai Tesque, Kyoto, Japan), and Antimycotic Mixed Stock Solution Penicillin 100 units/ml, Streptomycin 100 μg/ml, Amphotericin B 0.25 μg/ml (Nacalai Tesque, Kyoto, Japan). HuS-E/2 cells were cultured as previously described [10]. PHH were purchased from Gibco (Grand Island, NY, USA), the hepatocyte donor was a 58-year-old male who did not show any evidences of liver abnormalities. PHH were cultured

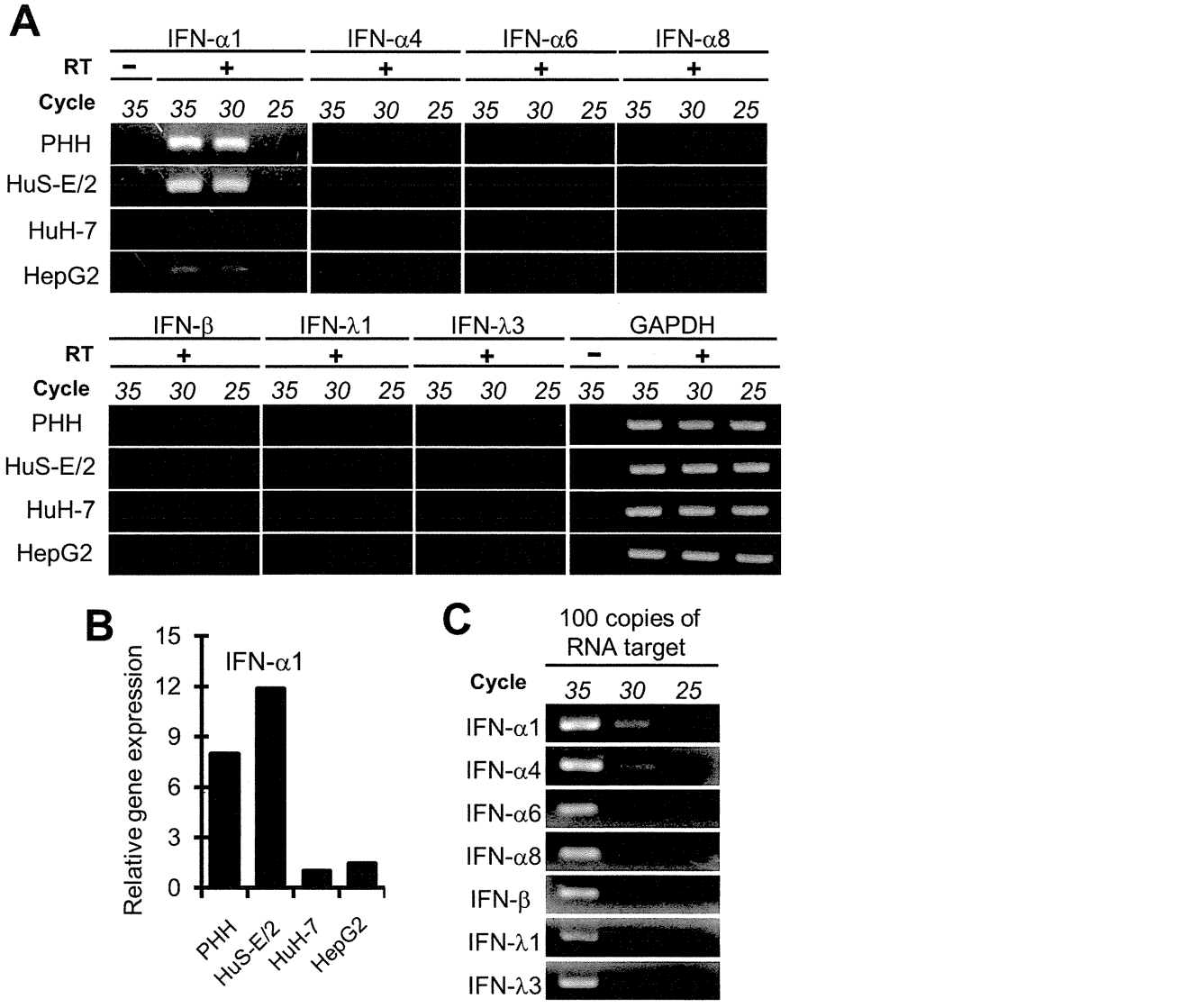

Figure 1. The expression of IFN-α1 gene in the cells derived from human hepatocytes. *A,* The expressions of several IFN genes in human hepatocyte derived cells. The presence of mRNAs for several IFN genes, IFN-α1, IFN-α4, IFN-α6, IFN-α8, IFN-β, IFN-λ1, and IFN-λ3, in PHH, HuS-E/2, HuH-7, and HepG2 cells without virus infection was examined by RT-PCR with different amplification cycles, 25, 30 and 35 cycles. RT-PCR was done with (+) or without (−) reverse transcriptase (RT) reaction. PCR products were separated in the agarose gel and stained with ethidium bromide. GAPDH mRNA was used as an internal standard substance. *B,* Semi-quantitative estimation of IFN-α1 mRNA in those cells. The relative amount of mRNA for IFN-α1 in those cells was estimated by qRT-PCR. The results of qRT-PCR were presented as relative gene expression using the RNA level of HuH-7 cells as a benchmark. *C.* Evaluation of sensitivity of RT-PCR system employed in the detection of IFN subtypes in small quantity. To show the sensitivity of RT-PCR system in this study, RT-PCR was performed with different amplification cycles, 25, 30 and 35 cycles using a primer set described in Table S1 and one hundred copies of in vitro synthesized RNA of each IFN subtype as a template.
doi:10.1371/journal.pone.0089869.g001

in serum-free hepatocyte maintenance medium (Gibco, NY, USA) for one week before starting each experiment.

Treatment with Neutralizing Antibodies (nAb) and Recombinant IFN

Two days prior to stimulation or infection, HuS-E/2 cells were seeded on the collagen coated 12 well plate (8×10^4 cells/well) to yield a confluent cell layer within 24 h. In the case of infection experiment, the cells were treated with nAb mentioned below for 12 hours (hrs). Then the cultured medium contained nAb were replaced with new culture medium containing Sendai virus (SeV) or cell culture derived recombinant HCV (HCVcc) after wash with phosphate buffer saline (PBS). SeV was prepared as described previously [10]. HCVcc was prepared from the HuH-7 or Huh-7.5 cells transfected with in vitro synthesized Jikei Fulminant Hepatitis (JFH) 1^{E2FL} RNA as described previously [11]. Recombinant human IFN-α was obtained from Merck (Darmstadt, Germany). Blocking Antibodies targeting IFN-α (MMHA-2), IFN-β (Rabbit polyclonal antibody), and IFNAR2 (MMHAR-2) were purchased from PBL Biomedical Laboratories (Piscataway, NJ).

RNA Extraction, Reverse-transcriptase Polymerase Chain Reaction (RT-PCR), and Quantitative RT-PCR (qRT-PCR)

Total RNA was isolated from cell cultures with Qiagen RNeasy Mini Kit (Qiagen GmbH, Hilden, Germany). Using 200 ng of total RNA as a template, RT-PCR was done with one-step RNA PCR kit (Takara, Kyoto, Japan) according to the manufacturer's instruction. qRT-PCR was performed with One Step SYBR PrimeScript PLUS RT-PCR Kit (Takara, Kyoto, Japan) by using 7500 Real-time PCR system (Applied Biosystems, Carlsbad CA) according to the manufacturer's instruction. The primer sets used in those PCRs are detailed in Table S1. Real-time PCR data are given as the mean of triplicate samples with standard deviation. The value obtained for the untreated control sample was generally set to 1.

Primer Design and Selection

The primers were designed based on the conserved specific sequence of IFN genes, using primer design software Primer-BLAST (National Center for Biotechnology Information. USA).

To evaluate the sensitivity and specificity of designed primer sets, RT-PCR using those primer sets and in vitro synthesized RNAs for subtypes of IFN as templates was performed. To make the in vitro expression plasmids for the IFNs, the cDNA fragment of each subtype of IFN was synthesized from total RNA from IFN-α stimulated HuS-E/2 cells by RT-PCR and subcloned in to the multiclonning sites of pcDNA3. The RNA fragment of each IFN subtype was synthesized with the plasmid in vitro using the MEGAscript T7 kit (Ambion, Austin, TX) according to the manufacturer's protocol. Synthesized RNA was treated with DNase I followed by acid phenol extraction to remove any remaining template DNA and used for RT-PCR by using one-step RNA PCR kit (Takara, Kyoto, Japan). The amplification conditions were 2 min preheating at 94°C, followed by from 25 to 35 cycles of 10 sec denaturation at 94°C, 30 sec annealing at 55°C, and 1 min elongation at 72°C.

Quantification of Type I IFN

Quantification of active type I IFN was performed by HEK-Blue IFN-α/β cells (Invivogen, San Diego, CA) according to the manufacturer's instruction. Type I IFN concentration (U/ml) was extrapolated from the linear range of a standard curve generated using known amounts of recombinant IFN-α (Merck Darmstadt, Germany).

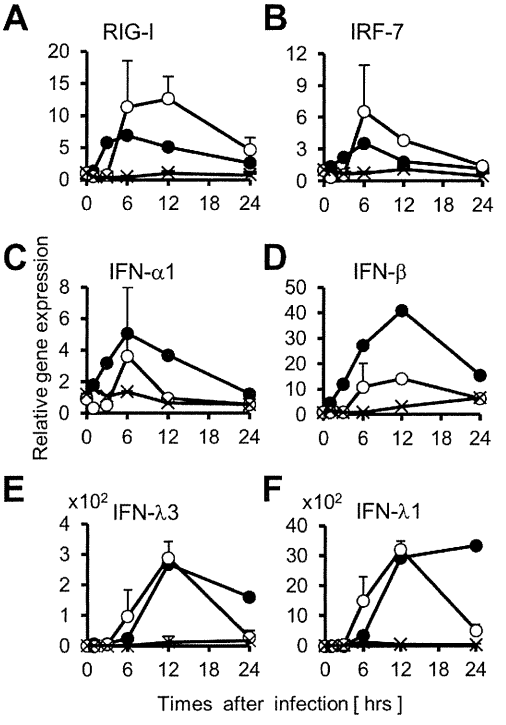

Figure 2. Expression profiles of genes associated with IFN signals in the cells after infection of SeV. Total RNAs were purified from PHH (closed circles), HuS-E/2 cells (open circles), and HuH-7 cells (cross marks) at indicated time points after infection of SeV. Relative quantities of RIG-I (*A*), IRF-7 (*B*), IFN-α1 (*C*), IFN-β (*D*), IFN-λ3 (*E*), and IFN-λ1 (*F*) mRNAs in each total RNA sample were examined by qRT-PCR and plotted using the RNA level firstly detected as a benchmark. The quantity of each RNA sample was normalized by the amount of GAPDH mRNA as relative gene expression. Error bars represent standard deviation (SD) of the mean of determinations from three experiments.
doi:10.1371/journal.pone.0089869.g002

Immunoblotting

Immunoblotting analysis was performed essentially as described previously [12], with slight modifications. Samples of cell lysates were prepared in lysis buffer (50 mM Tris-HCl (pH 8.0), 0.1% SDS, 0.5% sodium deoxycholate, 150 mM NaCl, 5 mM EDTA, 1 mM Orth vanadate (sigma-aldrich, St.Louis, USA), 10 mM NaF, Protease Inhibitor Cocktail (sigma-aldrich St.Louis, USA)). Antibodies used in this study were polyclonal rabbit antiserum against RIG-I at a 1:1000 dilution, IRF-7 at a 1:1000 dilution, STAT1 at a 1:1000 dilution, or p-STAT1 at a 1:1000 dilution. These antibodies were purchased from Cell Signaling Technology (Beverly, MA, USA). Immune-complexes were detected using Western Lightning reagent (PerkinElmer, Waltham, MA) by LAS-4000 system (Fujifilm, Tokyo, Japan).

ELISA for Human IFN-α Protein

Conditioned medium from culture system of HuS-E/2 cells infected with SeV, was collected at 3 and 12 hrs post-infection. The concentration of IFN-α in the conditioned medium was measured with human IFN-α enzyme-linked immunosorbent assay (ELISA) kit (PBL Biomedical Laboratories).

Indirect Immunofluorescence Analysis

Indirect immunofluorescence (IF) analysis was performed essentially as described previously [11]. The primary antibody was anti-SeV polyclonal antibody (1:200) (MBL International

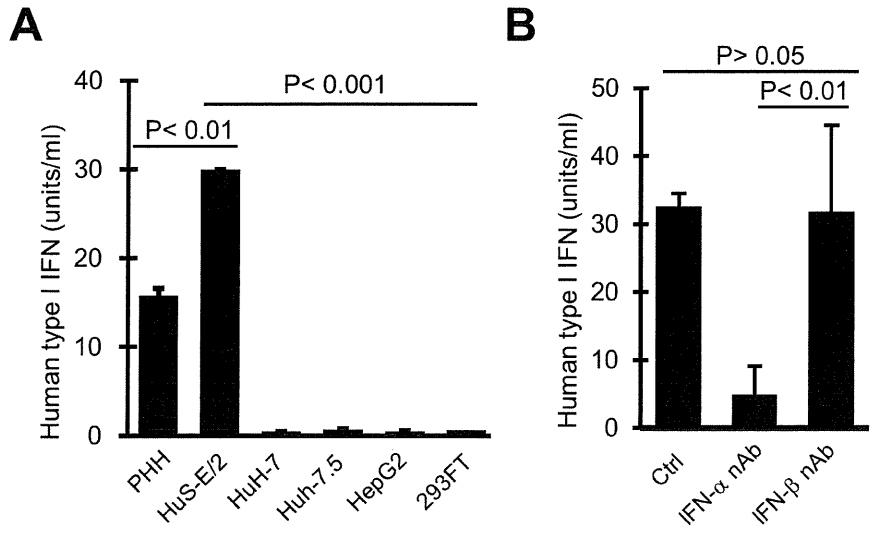

Figure 3. Activity of IFN-α constitutively produced into the culture medium. *A*, Activity of type I IFN produced from the cells without virus infection. Activities of type I IFN produced from PHH, HuS-E/2, HuH-7, Huh-7.5, HepG2, and 293FT cells in the culture media were examined by HEK-Blue™ IFN-α/β cells as described in experimental procedures section and plotted in the graph. *B*, Production of IFN-α from the cells without virus infection. Activity of type I IFN produced from HuS-E/2cells in the culture medium over night was examined as *A*, after treatment with 5 μg/ml neutralizing antibody (nAb) against IFN-α (IFN-α nAb) or IFN-β (IFN-β nAb) for 2 hrs. Error bars represent SD calculated from results of three independent experiments. Probability value (*P* value) was calculated with Student's t test.
doi:10.1371/journal.pone.0089869.g003

Corporation, MA, USA). The fluorescent secondary antibody was Alexa 568-conjugated anti-rabbit (Invitrogen, Carlsbad, CA). Nuclei were stained with 4′,6-diamidino-2-phenylindole (DAPI). The fluorescent signals were visualized by fluorescence microscopy (Bio Zero Keyence Co.).

Results

Induction of IFN Genes and ISGs in PHH and HuS-E/2 Cells by the Infection of Sendai Virus

We examined the antiviral responses of IFN system in some human hepatocyte derived cells against RNA viral infection using sendai virus (SeV) which is a negative strand RNA virus and has been widely used in studies on induction of IFN system [13]. The constitutive expression of IRF-3 and RIG-I genes was commonly found in all those cells as already repoted (data not shown, [10]). Our previous observation that IRF-7 gene was expressed in PHH and HuS-E/2 cells but not in HuH-7 cells under this condition was also confirmed (data not shown, [10]). In addition, the expression of IFN-α1 gene was newly observed in PHH and HuS-E/2 cells albeit at low level (Fig. 1*A*). That, however, was not in the case in HuH-7 and HepG2 cells, although the RT-PCR product was sometimes seen in HuH-7 and HepG2 cells but only vaguely (Fig. 1*A*). These results were also confirmed quantitatively by qRT-

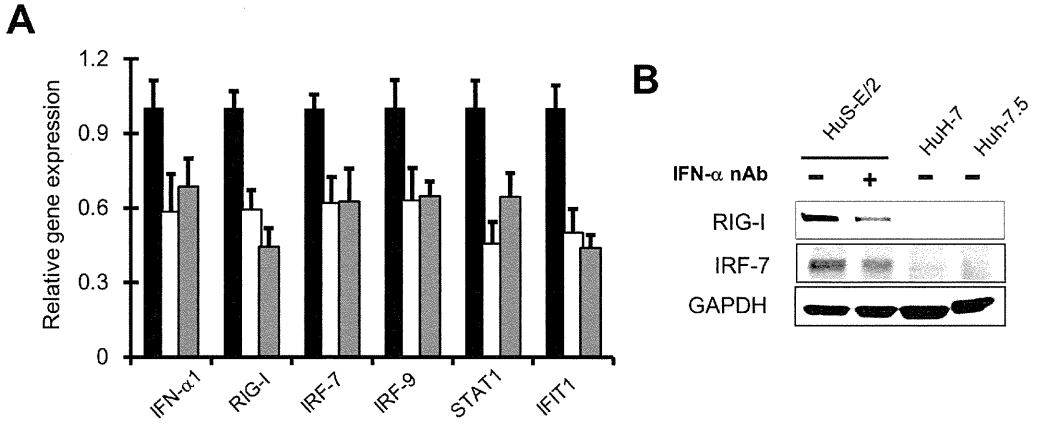

Figure 4. The function of constitutive IFN-α1 on the expression of the genes associated with IFN signals. *A*, The mRNA levels of the genes associated with IFN signals, RIG-I, IRF-7, IRF-9, STAT1, IFIT1, and IFN-α1 itself were examined in HuS-E/2 cells treated with and without nAb against IFN-α (IFN-α nAb, gray bars) (5 μg/ml) or IFNAR2 (IFNAR2 nAb, white bars) (5 μg/ml) for 12 hrs by qRT-PCR. Relative expression level of those genes are plotted using the RNA levels detected in the cells treated without nAb (Mock, black bars) as a benchmark. Results were derived from three independent experiments and error bars represent the calculated SD. *B*, Total cell lysates of HuS-E/2 cells treated with (+) or without (−) 5 μg/ml IFN-α nAb for 12 hrs were analyzed with immunoblotting using antibodies against RIG-I, and IRF-7. Those of HuH-7 and Huh-7.5 cells without treatment were also investigated. Protein levels was normalized among the samples by levels of GAPDH detected with anti-GAPDH antibody.
doi:10.1371/journal.pone.0089869.g004

PCR (Fig. 1*B*). In order to examine the gene expression of the other IFN subtypes in those cells, the primer sets for RT-PCR to detect mRNAs for those factors sensitively and specifically were designed and obtained to use for specific amplification of about one hundred copies of IFN-α4, IFN-α6, IFN-α8, IFN-β, IFN-λ1, or IFN-λ3 mRNAs (Fig. 1*C* and Table S1). Those mRNAs, however, were not detected at all in all cells used in this study by this RT-PCR condition (Fig. 1*A*). These results suggested that IFN-α, at least IFN-α1, but not IFN-β and IFN–λ, is slightly produced in human hepatocytes without virus infection.

Next, the effect of SeV infection on mRNA levels of those genes was investigated in those cells. The mRNA levels of IRF-7 and IFN-α1, a target gene product of IRF-7, were transiently increased and reached peaks 6 hrs post-infection (p.i.) in both PHH and HuS-E/2 cells (Fig. 2*B and 2C*, closed and open circles). Those of IFN-β, and IFN-λ3 reached peaks 12 hrs p.i. in those cells in similar ways (Fig. 2*D and 2E*, open and closed circles). IFN-λ1 mRNA was also increased by 12 hrs p.i. in both HuS-E/2 cells and PHH (Fig. 2*F*, open and closed circles). It decreased from 12 to 24 hrs p.i. in HuS-E/2 cells (Fig. 2*F*, open circles) whereas it slightly increased in PHH (Fig. 2*F*, closed circles). The gene expression of RIG-I, a key factor in the innate immune response to RNA virus infection in many cells [14,15], was also investigated. The increase of RIG-I mRNA was observed from 1 hr to 6 hrs p.i. in PHH (Fig. 2*A*, closed circles). Although that was observed from 3 hrs to 12 hrs p.i., the similar pattern of the increase was observed in HuS-E/2 cells (Fig. 2*A*, open circles). The expressions of RIG-I, IRF-7, and IFNs genes were also assessed in HuH-7 cells following infection. Obvious increase of those mRNAs, however, was not detected in telling contrast to PHH and HuS-E/2 cells (Fig. 2, crosses). These observations indicated that this early innate immune response to SeV infection did not occur in HuH-7 cells. The absence of this early response may explain why HuH-7 cells support efficient proliferation of recombinant HCV [16]. On the other hand, the innate immune response of HuS-E/2 cells against SeV infection seemed to be relatively similar to that of PHH, although the responsiveness curves of those gene expression were slightly different. Thus, we supporsed that HuS-E/2 cells provide a valuable model for studying innate immune response of human hepatocytes against viral infection.

Active IFN-α was Constitutively Produced in HuS-E/2 Cells at a Low Level

In this study, we addressed the constitutive expression of IFN-α1 gene observed in PHH and HuS-E/2 cells, since the detection of IFN-α1 mRNA in the liver tissues from normal human individuals was already detected by RNA blot hybridization, but its function was not cleared yet [8].

The presence of IFN-α in the conditioned medium from HuS-E/2 cell culture system was examined firstly by the ELISA system for IFN-α. However, that was not detected probably because of low concentration of secreted IFN-α and low sensitivity of the system. Then the activity of type I IFN in the culture medium assessed by using HEK-Blue type I IFN assay system in which the cells are designed to produce embryonic alkaline phosphatase protein in type I IFN receptor signaling-dependent manner. As shown in Fig. 3*A*, the culture medium from HuS-E/2 cell culture system showed significantly higher activity of type I IFN than those from the culture systems for Huh-7.5, HuH-7, and HepG2 cells as well as 293FT cells, a cell line derived from human embryonic kidney. To confirm above results further, the effect of neutralizing antibody (nAb) targeting IFN-α on the above conditioned medium was examined similarly. As shown in Fig. 3*B*, the pretreatment of the conditioned medium from HuS-E/2 cell culture with this antibody effectively suppressed the activity of IFN receptor signaling, while nAb targeting IFN-β did not affected (Fig.3*B*). These observations indicated that functional type I IFN was included in the conditioned medium from HuS-E/2 cell culture system and, at least, the majority of the type I IFN in the medium was IFN-α and not IFN-β. From above results, we concluded that HuS-E/2 cells produce functional IFN-α into the culture medium without virus infection.

The Basal Expression of IFN-α1 and ISGs was Elevated by Type I IFN Receptor Signaling

To see whether the IFN-α1 produced in the cells without virus infection affects the cells through the autocrine or paracrine signaling regardless of low level production, the basal expression of several ISGs in HuS-E/2 cells cultured in the medium containing nAb targeting IFNα/β receptor (IFNAR) 2, one of the receptors for type I IFN, were investigated. As shown in Fig. 4*A*, it was clearly observed that the mRNA levels of RIG-I, IRF-7, IRF-9, signal transducer and activator of transcription (STAT) 1, and IFN-induced protein with Tetratricopeptide 1 (IFIT1) were diminished in the cells with the nAb treatment, compared to mock treated cells. Quite similar results were observed in the cells treated with nAb targeting IFN-α (data not shown). The basal expression level of IFN-α1 gene was also reduced by these treatments (Fig. 4*A*). Decreased protein levels of RIG-I and IRF-7 were also observed in HuS-E/2 cells treated with nAb targeting IFN-α, while these proteins were below the detectable level in HuH-7 and Huh-7.5 cells as predicted (Fig. 4*B*). As the treatments of two different nAbs showed the similar results to each other, it was suggested that the type I IFN receptor signaling upregulates the expression of those ISGs, as well as IFN-α1 gene, in basal level in HuS-E/2 cells to some extent.

Basal Production of IFN-α in HuS-E/2 Cells Contributes to Rapid Antiviral Response during Early Phase of Infection

To study the functional role of basal level production of IFN-α in HuS-E/2 cells, the innate immune responses of the cells treated with the above nAbs against the RNA virus infection was investigated. In this experiment, HuS-E/2 cells pretreated with nAbs for 12 hrs to interrupt the basal IFN signaling were exposed to the fresh culture medium contained SeV for 30 min after rinsing the nAbs off from the cells. After the infection, the cells were cultured for 3 hrs and then used as follows (Fig. 5*A*). As the induced expression of RIG-I gene, used as a representative of ISGs, by the treatment with recombinant IFN-α was observed similarly in both cells pretreated with and without nAbs (Fig. 5*B*), it was clearly shown that the cells pretreated with the nAbs retained responsiveness to IFN-α rinsing procedure. At first, the levels of mRNAs for RIG-I, IRF-7, IFN-α1, IFN-β, IFN-λ1, and IFN-λ3 were examined in the cells with or without SeV infection. As shown in Fig. 5*C*, almost the similar patterns of increases of those mRNAs were observed in the cells with SeV infection, although only minor levels of the induction were found in the cases of IRF-7 and IFN-α mRNAs even in the mock pretreated cells. In all the cases, nAb pretreatments effectively suppressed the increases of those mRNAs 3 hrs after SeV infection (Fig. 5*C*). As shown in Fig. 5*D*, the suppression of IFN-α protein production in the culture medium 12 hrs after the infection was also observed by using ELISA.

Next, to examine the effect of the pretreatments with nAbs on virus-induced STAT1 activation, phosphorylated form of STAT1, activated form of STAT1, was detected in SeV infected cells pretreated with nAbs by western blot analysis using anti-

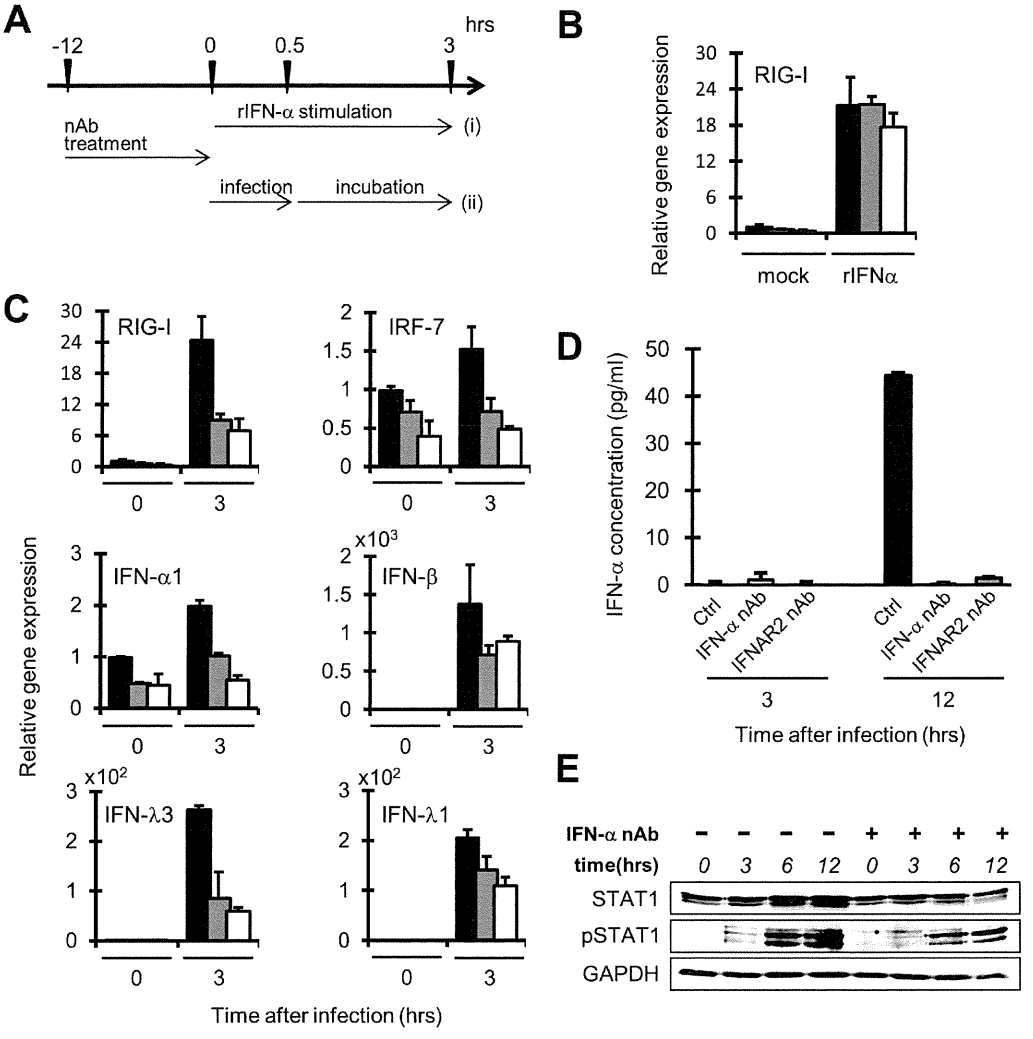

Figure 5. Roles of Constitutive IFN-α on the virus-induced antiviral responses in HuS-E/2 cells. *A*, Schematic of the time schedules for the experiments of recombinant human IFN-α (rIFN-α treatment (i) or SeV infection (ii) after nAb treatment. *B*, Responses of the cells pretreated with IFN-α or IFNAR2 nAbs against exogenous stimulation of rIFN-α. RIG-I mRNA in the cells treated with rIFN-α (2.5 unit/ml) (i) for 0 and 3 hrs after the treatment with IFNAR2 nAb (gray bars), IFN-α nAb (white bars) or mock (black bars) were analyzed by qRT-PCR. Relative expression level of those genes are plotted using each RNA level detected in the cells treated with mock for 0 hr as a benchmark (*B, C*). Error bars represent the calculated SD from the results obtained in three independent experiments (*B, C, D*). *C*, Responses of the cells pretreated with IFN-α or IFNAR2 nAbs against SeV infection. IFN-α1, IFN-β, IFN-λ1, IFN-λ3, and IRF-7 mRNAs in the cells processed as described for panel *B* except infection of SeV (ii) instead of rIFN-α treatment, were analyzed by qRT-PCR. *D*, SeV infection induced IFN-α production from the cells pretreated with IFN-α or IFNAR2 nAbs. Quantity of IFN-α protein in the culture medium was determined by ELISA at 3 and 12 hrs post-infection of SeV. The cells were processed as described for panels *C. E.* STAT1 phosphorylation in the cells pretreated with IFN-α nAbs after SeV infection. The phosphorylation status of STAT1 in the cells processed as described for panel *D* except pretreatment with (+) or without (−) IFN-α nAb only was analyzed by western blot analysis using anti-STAT1 antibody (STAT1), anti-phosphorylated STAT1 antibody (pSTAT1) at 3, 6, and 12 hrs post-infection of SeV. Protein levels were normalized among the samples by levels of GAPDH detected with anti-GAPDH antibody.
doi:10.1371/journal.pone.0089869.g005

phosphorylated STAT1 (pSTAT1). As shown in Fig. 5*E*, the level of pSTAT1 found in the SeV infected cells without IFN-α nAb pretreatment was apparently reduced in the cells with pretreatment at 3, 6 and 12 hrs post-infection, although the protein levels of STAT1 were not affected by the pretreatment, suggesting that pretreatment by IFN-α nAb suppressed the IFN signaling induced by virus infection.

These results suggested that IFN-α produced in the HuS-E/2 cells without virus infection plays a role in the enhancement of initial response of IFN system.

IFN-α Released from HuS-E/2 cells without Viral Infection Contributes to Inhibit Initial Infection and Proliferation of RNA Viruses, Including HCV

To examine whether IFN-α produced in the cells without virus infection actually plays a role in prevention of viral infection, the permissiveness of HuS-E/2 cells, which were pretreated with and without IFNAR2 nAb, against SeV infection was investigated. Compared to the cells without pretreatment of nAb (shown as control panels in Fig. 6*A*), the number of SeV infected cells (shown in red) was increased in the cells with treatment both 6 and 9 hrs after infection in time-dependent manner (Fig. 6*B*). We also assessed

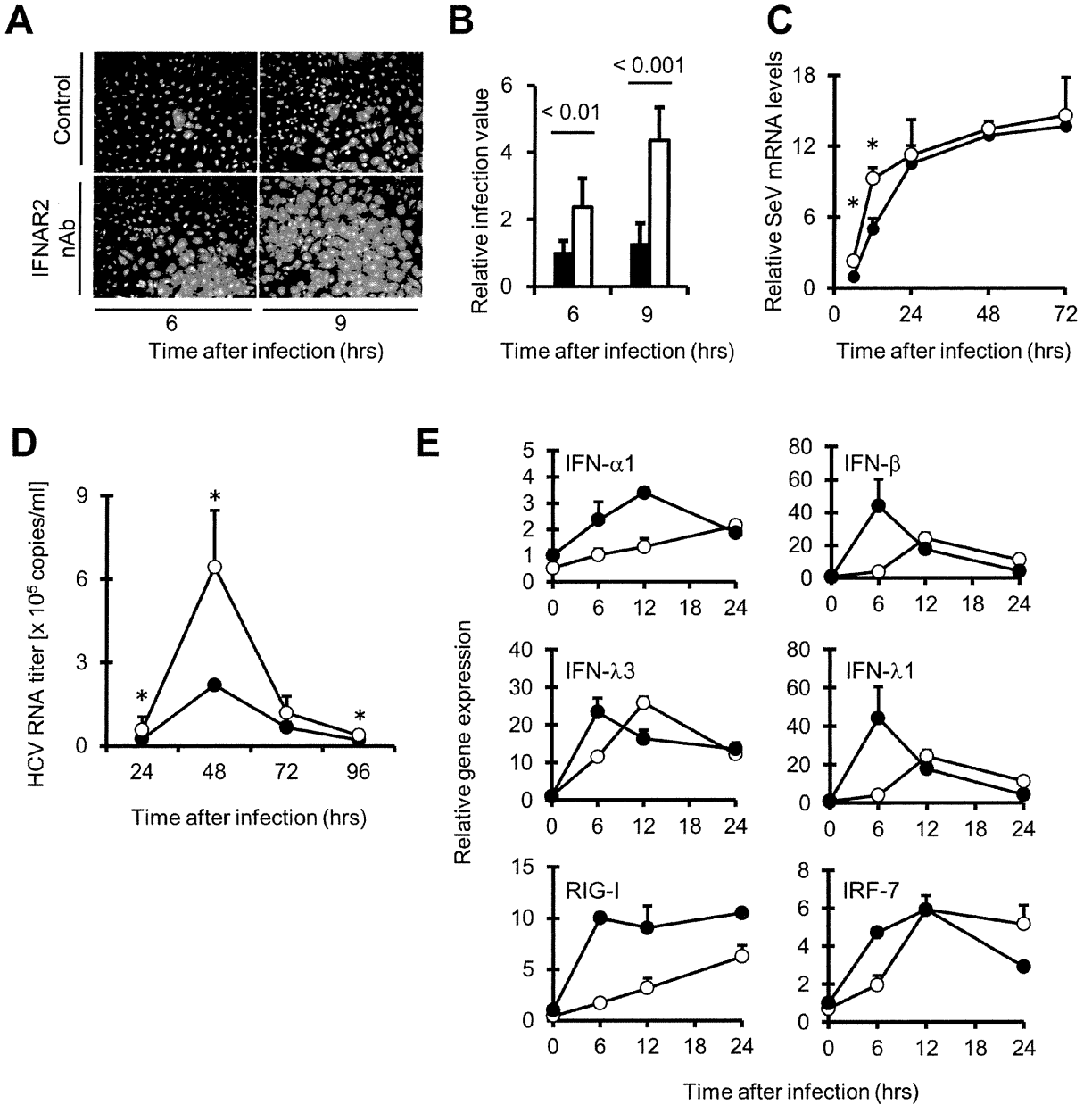

Figure 6. Suppressive role of constitutive IFN-α on viral infection or initial viral proliferation. *A*, Enhanced infection of SeV by neutralization of constitutive IFN-α visualized with IF. Cells were processed basically as described in the figure legend for Fig. 5, panel *C* (*A, B, C, D, E*). At 6 and 9 hrs after SeV infection, the cells were fixed and studied by IF using anti SeV antibodies (red). Nuclei were stained with DAPI (blue). *B*, Numerical conversion of the results in panel *A*. Infection of SeV was quantified by counting of the fluorescent positive cells in ten fields of views per well of two wells. Relative infection values of the cells treated with (white bars) and without (black bars) IFNAR2 nAb were calculated by using the averaged number of infected cells without nAb treatment at 6 hrs postinfection as a benchmark. *P* value was calculated with Student's t test. *C*, Quantification of SeV RNA were measured by qRT-PCR. RNA samples from HuS-E/2 cells pre-treated with (open circles) and without (closed circles) nAb against IFN-α (5 μg/ml) were prepared at the indicated time points (24, 48, and 72 hrs post-infection with SeV). *D*, HCV RNA copies in HuS-E/2 cells pre-treated with (open circles) and without (closed circles) IFN-α nAb at the indicated time points (24, 48, 72, and 96 hrs post-infection with HCVcc) were measured by qRT-PCR. *E*, Time course expression of IFN-α1, IFN-β, IFN-λ1, IFN-λ3, RIG-I and IRF-7 mRNAs in the cells pre-treated with (open circles) or without (closed circles) IFN-α nAb during early stage of HCV infection (6, 12, 18, and 24 hrs post-infection with HCVcc). For each analysis, the results are normalized to the value obtained from the mock treatment. Error bars represent the calculated SD from the results obtained in three independent experiments (*B, C, D, E*).
doi:10.1371/journal.pone.0089869.g006

the proliferation of SeV in HuS-E/2 cells with or without pretreatment of IFN-α nAb by quantitative estimation of SeV genomic RNA. As shown in Fig. 6*C*, the increase of SeV genomic RNA levels was clearly observed in the cells with the pre-treatment at 12 hrs post-infection, suggesting that the preexisting IFN-α play a suppressive role on SeV proliferation during early phase of infection. In addition, to investigate the effect of constitutive IFN-α on the hepatotropic virus, we examined the infection and proliferation of HCVcc in HuS-E/2 cells with or without pretreatment of IFN-α nAb. As shown in Fig. 6*D*, the transient

infection and proliferation of HCVcc was observed in the HuS-E/2 cells as previously reported [10]. It was clearly observed that HCV RNA levels in the cells with the pretreatment were significantly higher than the cells without pretreatment from 24 to 48 hrs post-infection, although the significant difference was not observed in each cells from 72 to 96 hrs post-infection (Fig. 6*D*). Next, the expression of several IFN related genes in HuS-E/2 cells with or without the pretreatment was examined after HCVcc infection. As shown in Fig. 6*E*, compared to the cells without pretreatment, the delayed increases of RNAs for IFN-α1, IFN-β, IFN-λ1, IFN-λ3, RIG-I and IRF-7 after HCV infection were observed in HuS-E/2 cells with the pretreatment, although induction patterns were varied among those genes. These results suggested that IFN-α produced from HuS-E/2 cells without virus infection contributes to rapid antiviral innate immune response of the cells to limit the proliferation of HCV during the initial stage of infection.

Discussion

In this study, we showed that IFN-α1 gene is expressed in HuS-E/2 cells without virus infection as in the case of PHH, albeit at a low level and that the IFN-α, including IFN-α1, functions to elevate the expression of the genes related with anti-viral innate immune system in the cells. Previously, the expression pattern of the genes related with innate immunity of the HuS-E/2 cells, was shown to be similar to that of PHH [10]. The constitutive expression of IFN-α1 gene was also previously observed in human liver tissue [8]. Our results, therefore, suggested that the previous detection of IFN-α1 mRNA in normal human liver is due in part at least to the gene expression in hepatocytes in that tissue. The constitutive production of type I IFN has been reported previously in several tissues mainly concerning IFN-β [17,18,19,20]. The mechanisms that support the constitutive production of IFN-β have been relatively studied well and revealed to be involved with multiple transcription factors, such as c-Jun and RelA [6]. However, molecular mechanism that controls the steady-state production of IFN-α has been largely unclear. The transcriptional promoter region of IFN-α1 gene contains two regulatory elements, one is homologous to the positive regulatory domain I (PRDI) of the IFN-β gene promoter [21,22,23] and another is virus-responsive enhancer module, as proposed to a TG-like domain [24,25]. Our previous report showed that IRF-7 gene is constitutively expressed in HuS-E/2 cells [10]. IRF-7, together with IRF-3, is known to play a pivotal role in the induction of IFN-α and IFN-β genes through binding with PRDI in cells infected with virus [3,4], although it was suggested that IRF-7, rather than IRF-3, is important to suppress the infection and replication of HCV in the cells [10]. The basal expression of IFN-α and IFN-β genes, however, was reported not to depend on these regulatory factors [26]. We also observed that silencing IRF-7 in HuS-E/2 cells with shRNA method did not diminish the steady-state level expression of IFN-α1 (data not shown). We found some sequences homologous to the binding sites for some hepatocyte-specific transcription factors, including hepatocyte nuclear factor 1α (HNF1α), HNF1β, and HNF4α within the region 5000 base pairs upstream of the transcription start site of IFN-α1 gene using computational promoter analysis (data not shown). It, therefore, may be possible that the tissue-specific transcription factor contributes to the expression of IFN-α1 gene in a tissue-specific manner. As a recent study showed that tissue–specific differences in IFN genes or ISG expression can be attributed in part to the epigenetic regulation [27], it is probable that the innate immune phenotypes of IFN-α gene in human hepatocytes is also associated with tissue-specific patterns of histone modification. Further study is needed to clarify the molecular mechanisms of constitutive expression of IFN-α1 gene in human hepatocytes.

The results obtained from this study showed the functional role of the constitutive IFN-α in human hepatocytes on the immediate innate immune response against RNA virus infection, including HCV, through augmentation of the steady-state level expression of several genes related to detection of the infection and induction of IFN systems, such as RIG-I, IRF-7, and IFNs genes. Rapid activation of IFN system should be important to suppress the expansion of viral infection. The constitutive IFN-β has been reported previously in several tissues and was demonstrated to strengthen IFN response toward viral infection [17,18,19,20]. This constitutive IFN-β involves a positive feedback loop as proposed in a "revving-up model" in such tissues [28]. The weak cellular signals constantly introduced by constitutive IFN-β allows cells to elicit a more robust response against viral infection than the cells without such signals [17]. This signaling likely occasion induction of the IRF-7 gene without viral infection as a priming effect [29]. Cardiac myocytes was reported to produce higher basal IRF-7 without viral infection through the Jak-STAT pathway activated with preexisting IFN-β for instant antiviral response [20]. Plasmacytoid dendritic cells (pDCs) are known to produce IFN-α and IRF-7 constitutively just like human hepatocytes reported in this study. pDCs respond rapidly and effectively to a range of viral pathogens with high production of IFN-α in constitutive IRF-7 production dependent manner [30,31,32]. These suggested that IRF7, of which gene expression is induced by constitutive type-I interferon, both IFN-α and IFN-β, in those cells, plays a crucial role in the priming effect on the consecutive and rapid anti-viral innate immune response.

The liver is the largest solid organ in the body with dual inputs for its blood supply. It receives 80% of its blood supply from the gut through the portal vein, which is rich in bacterial products, environment toxins, and food borne pathogens. The remaining 20% of the blood is supplied from vascularization by the hepatic artery [33]. This high exposure to pathogens may require that the liver has an efficient and rapid defensive mechanism against possible frequent infection. Although most pathogens that get at the liver are killed by local innate and adaptive immune responses, hepatitis viruses (such as HBV and HCV) which gain the ingenious function to escape immune control persist in hepatocytes [34,35,36,37,38]. Therefore, further study to reveal the role of steady-state production of IFN-α1 in human hepatocytes may provide new insights into the virus-cell interaction and chronic infection of hepatotropic viruses.

In addition to the importance for the antiviral effect, it has been also proposed that the constitutive IFN-β primes for an efficient subsequent response to other cytokines and are also important for immune homeostasis [39,40,41], maintenance of bone density [42] and antitumor immunity [43]. Further analysis of the possible role of constitutive IFN-α on the other physiological events in human hepatocytes may be required.

Supporting Information

Table S1 List of names and sequences of the primers and expected sizes of RT-PCR products using those primers.
(TIF)

Author Contributions

Conceived and designed the experiments: YT MH. Performed the experiments: YT HK. Analyzed the data: YT MH. Contributed reagents/materials/analysis tools: TF KS MH. Wrote the paper: YT MH.

References

1. Samuel CE (2001) Antiviral actions of interferons. Clin Microbiol Rev 14: 778–809, table of contents.
2. Randall RE, Goodbourn S (2008) Interferons and viruses: an interplay between induction, signalling, antiviral responses and virus countermeasures. J Gen Virol 89: 1–47.
3. Yoneyama M, Fujita T (2010) Recognition of viral nucleic acids in innate immunity. Rev Med Virol 20: 4–22.
4. Matsumiya T, Imaizumi T, Yoshida H, Satoh K (2011) Antiviral signaling through retinoic acid-inducible gene-I-like receptors. Arch Immunol Ther Exp (Warsz) 59: 41–48.
5. Katze MG, He Y, Gale M, Jr. (2002) Viruses and interferon: a fight for supremacy. Nat Rev Immunol 2: 675–687.
6. Gough DJ, Messina NL, Clarke CJ, Johnstone RW, Levy DE (2012) Constitutive type I interferon modulates homeostatic balance through tonic signaling. Immunity 36: 166–174.
7. Pestka S, Krause CD, Walter MR (2004) Interferons, interferon-like cytokines, and their receptors. Immunol Rev 202: 8–32.
8. Tovey MG, Streuli M, Gresser I, Gugenheim J, Blanchard B, et al. (1987) Interferon messenger RNA is produced constitutively in the organs of normal individuals. Proc Natl Acad Sci U S A 84: 5038–5042.
9. Aly HH, Qi Y, Atsuzawa K, Usuda N, Takada Y, et al. (2009) Strain-dependent viral dynamics and virus-cell interactions in a novel in vitro system supporting the life cycle of blood-borne hepatitis C virus. Hepatology 50: 689–696.
10. Aly HH, Watashi K, Hijikata M, Kaneko H, Takada Y, et al. (2007) Serum-derived hepatitis C virus infectivity in interferon regulatory factor-7-suppressed human primary hepatocytes. J Hepatol 46: 26–36.
11. Miyanari Y, Atsuzawa K, Usuda N, Watashi K, Hishiki T, et al. (2007) The lipid droplet is an important organelle for hepatitis C virus production. Nat Cell Biol 9: 1089–1097.
12. Kushima Y, Wakita T, Hijikata M (2009) A disulfide-bonded dimer of the core protein of hepatitis C virus is important for virus-like particle production. J Virol 84: 9118–9127.
13. Maeno K, Yoshii S, Nagata I, Matsumoto T (1966) Growth of Newcastle disease virus in a HVJ carrier culture of HeLa cells. Virology 29: 255–263.
14. Kato H, Takeuchi O, Sato S, Yoneyama M, Yamamoto M, et al. (2006) Differential roles of MDA5 and RIG-I helicases in the recognition of RNA viruses. Nature 441: 101–105.
15. Kato H, Sato S, Yoneyama M, Yamamoto M, Uematsu S, et al. (2005) Cell type-specific involvement of RIG-I in antiviral response. Immunity 23: 19–28.
16. Blight KJ, McKeating JA, Rice CM (2002) Highly permissive cell lines for subgenomic and genomic hepatitis C virus RNA replication. J Virol 76: 13001–13014.
17. Sato M, Suemori H, Hata N, Asagiri M, Ogasawara K, et al. (2000) Distinct and essential roles of transcription factors IRF-3 and IRF-7 in response to viruses for IFN-alpha/beta gene induction. Immunity 13: 539–548.
18. Lienenklaus S, Cornitescu M, Zietara N, Lyszkiewicz M, Gekara N, et al. (2009) Novel reporter mouse reveals constitutive and inflammatory expression of IFN-beta in vivo. J Immunol 183: 3229–3236.
19. Hsu AC, Parsons K, Barr I, Lowther S, Middleton D, et al. (2012) Critical role of constitutive type I interferon response in bronchial epithelial cell to influenza infection. PLoS One 7: e32947.
20. Zurney J, Howard KE, Sherry B (2007) Basal expression levels of IFNAR and Jak-STAT components are determinants of cell-type-specific differences in cardiac antiviral responses. J Virol 81: 13668–13680.
21. Keller AD, Maniatis T (1988) Identification of an inducible factor that binds to a positive regulatory element of the human beta-interferon gene. Proc Natl Acad Sci U S A 85: 3309–3313.
22. Braganca J, Civas A (1998) Type I interferon gene expression: differential expression of IFN-A genes induced by viruses and double-stranded RNA. Biochimie 80: 673–687.
23. Goodbourn S, Maniatis T (1988) Overlapping positive and negative regulatory domains of the human beta-interferon gene. Proc Natl Acad Sci U S A 85: 1447–1451.
24. Genin P, Braganca J, Darracq N, Doly J, Civas A (1995) A novel PRD I and TG binding activity involved in virus-induced transcription of IFN-A genes. Nucleic Acids Res 23: 5055–5063.
25. MacDonald NJ, Kuhl D, Maguire D, Naf D, Gallant P, et al. (1990) Different pathways mediate virus inducibility of the human IFN-alpha 1 and IFN-beta genes. Cell 60: 767–779.
26. Hata N, Sato M, Takaoka A, Asagiri M, Tanaka N, et al. (2001) Constitutive IFN-alpha/beta signal for efficient IFN-alpha/beta gene induction by virus. Biochem Biophys Res Commun 285: 518–525.
27. Fang TC, Schaefer U, Mecklenbrauker I, Stienen A, Dewell S, et al. (2012) Histone H3 lysine 9 di-methylation as an epigenetic signature of the interferon response. J Exp Med 209: 661–669.
28. Levy DE, Marie I, Smith E, Prakash A (2002) Enhancement and diversification of IFN induction by IRF-7-mediated positive feedback. J Interferon Cytokine Res 22: 87–93.
29. Taniguchi T, Takaoka A (2001) A weak signal for strong responses: interferon-alpha/beta revisited. Nat Rev Mol Cell Biol 2: 378–386.
30. Izaguirre A, Barnes BJ, Amrute S, Yeow WS, Megjugorac N, et al. (2003) Comparative analysis of IRF and IFN-alpha expression in human plasmacytoid and monocyte-derived dendritic cells. J Leukoc Biol 74: 1125–1138.
31. Kerkmann M, Rothenfusser S, Hornung V, Towarowski A, Wagner M, et al. (2003) Activation with CpG-A and CpG-B oligonucleotides reveals two distinct regulatory pathways of type I IFN synthesis in human plasmacytoid dendritic cells. J Immunol 170: 4465–4474.
32. Colantonio AD, Epeldegui M, Jesiak M, Jachimowski L, Blom B, et al. (2011) IFN-alpha is constitutively expressed in the human thymus, but not in peripheral lymphoid organs. PLoS One 6: e24252.
33. Zufferey R, Nagy D, Mandel RJ, Naldini L, Trono D (1997) Multiply attenuated lentiviral vector achieves efficient gene delivery in vivo. Nat Biotechnol 15: 871–875.
34. von Hahn T, Yoon JC, Alter H, Rice CM, Rehermann B, et al. (2007) Hepatitis C virus continuously escapes from neutralizing antibody and T-cell responses during chronic infection in vivo. Gastroenterology 132: 667–678.
35. Gale M, Jr., Foy EM (2005) Evasion of intracellular host defence by hepatitis C virus. Nature 436: 939–945.
36. Li XD, Sun L, Seth RB, Pineda G, Chen ZJ (2005) Hepatitis C virus protease NS3/4A cleaves mitochondrial antiviral signaling protein off the mitochondria to evade innate immunity. Proc Natl Acad Sci U S A 102: 17717–17722.
37. Meylan E, Curran J, Hofmann K, Moradpour D, Binder M, et al. (2005) Cardif is an adaptor protein in the RIG-I antiviral pathway and is targeted by hepatitis C virus. Nature 437: 1167–1172.
38. Foy E, Li K, Wang C, Sumpter R, Jr., Ikeda M, et al. (2003) Regulation of interferon regulatory factor-3 by the hepatitis C virus serine protease. Science 300: 1145–1148.
39. Swann JB, Hayakawa Y, Zerafa N, Sheehan KC, Scott B, et al. (2007) Type I IFN contributes to NK cell homeostasis, activation, and antitumor function. J Immunol 178: 7540–7549.
40. Honda K, Sakaguchi S, Nakajima C, Watanabe A, Yanai H, et al. (2003) Selective contribution of IFN-alpha/beta signaling to the maturation of dendritic cells induced by double-stranded RNA or viral infection. Proc Natl Acad Sci U S A 100: 10872–10877.
41. Musso G, Gambino R, Cassader M (2011) Interactions between gut microbiota and host metabolism predisposing to obesity and diabetes. Annu Rev Med 62: 361–380.
42. Takayanagi H, Kim S, Matsuo K, Suzuki H, Suzuki T, et al. (2002) RANKL maintains bone homeostasis through c-Fos-dependent induction of interferon-beta. Nature 416: 744–749.
43. Jablonska J, Leschner S, Westphal K, Lienenklaus S, Weiss S (2010) Neutrophils responsive to endogenous IFN-beta regulate tumor angiogenesis and growth in a mouse tumor model. J Clin Invest 120: 1151–1164.

JVI
Journals.ASM.org

Japanese Encephalitis Virus Core Protein Inhibits Stress Granule Formation through an Interaction with Caprin-1 and Facilitates Viral Propagation

Hiroshi Katoh,[a] Toru Okamoto,[a] Takasuke Fukuhara,[a] Hiroto Kambara,[a] Eiji Morita,[b] Yoshio Mori,[d] Wataru Kamitani,[c] Yoshiharu Matsuura[a]

Department of Molecular Virology,[a] International Research Center for Infectious Diseases,[b] and Global COE Program,[c] Research Institute for Microbial Diseases, Osaka University, Osaka, Japan; Department of Virology III, National Institute of Infectious Diseases, Tokyo, Japan[d]

Stress granules (SGs) are cytoplasmic foci composed of stalled translation preinitiation complexes induced by environmental stress stimuli, including viral infection. Since viral propagation completely depends on the host translational machinery, many viruses have evolved to circumvent the induction of SGs or co-opt SG components. In this study, we found that expression of Japanese encephalitis virus (JEV) core protein inhibits SG formation. Caprin-1 was identified as a binding partner of the core protein by an affinity capture mass spectrometry analysis. Alanine scanning mutagenesis revealed that Lys^{97} and Arg^{98} in the α-helix of the JEV core protein play a crucial role in the interaction with Caprin-1. In cells infected with a mutant JEV in which Lys^{97} and Arg^{98} were replaced with alanines in the core protein, the inhibition of SG formation was abrogated, and viral propagation was impaired. Furthermore, the mutant JEV exhibited attenuated virulence in mice. These results suggest that the JEV core protein circumvents translational shutoff by inhibiting SG formation through an interaction with Caprin-1 and facilitates viral propagation *in vitro* and *in vivo*.

In eukaryotic cells, environmental stresses such as heat shock, oxidative stress, UV irradiation, and viral infection trigger a sudden translational arrest, leading to stress granule (SG) formation (1). SGs are cytoplasmic foci composed of stalled translation preinitiation complexes and are postulated to play a critical role in regulating mRNA metabolism during stress via so-called "mRNA triage" (2). The initiation of SG formation results from phosphorylation of eukaryotic translation initiation factor 2α (eIF2α) at Ser^{51} by various kinases, including protein kinase R (PKR), PKR-like endoplasmic reticulum kinase (PERK), general control nonrepressed 2 (GCN2), and heme-regulated translation inhibitor (HRI), which are commonly activated by double-stranded RNA (dsRNA), endoplasmic reticulum (ER) stress, nutrient starvation, and oxidative stress, respectively. Phosphorylation of eIF2α reduces the amount of eIF2-GTP-tRNA complex and inhibits translation initiation, leading to runoff of elongating ribosomes from mRNA transcripts and the accumulation of stalled translation preinitiation complexes. Thus, SGs are defined by the presence of components of translation initiation machinery, including 40S ribosome subunits, poly(A)-binding protein (PABP), eIF2, eIF3, eIF4A, eIF4E, eIF4G, and eIF5. Then, primary aggregation occurs through several RNA-binding proteins (RBPs), including T-cell intracellular antigen-1 (TIA-1), TIA-1-related protein 1 (TIAR), and Ras-Gap-SH3 domain-binding protein (G3BP). These RBPs are independently self-oligomerized with the stalled initiation factors and with other RBPs, such as USP10, hnRNP Q, cytoplasmic activation/proliferation-associated protein-1 (Caprin-1), and Staufen and with nucleated mRNA-protein complex (mRNP) aggregations (3, 4). SG assembly begins with the simultaneous formation of numerous small mRNP granules which then progressively fuse into larger and fewer structures, a process known as secondary aggregation (5). The aggregation of TIA-1 or TIAR is regulated by molecular chaperones, such as heat shock protein 70 (Hsp70) (3), whereas that of G3BP is controlled by its phosphorylation at Ser^{149} (4). SG formation and disassembly in response to cellular stresses are strictly regulated by multiple factors.

Viral infection can certainly be viewed as a stressor for cells, and SGs have been reported in some virus-infected cells. Since the propagation of viruses is completely reliant on the host translational machinery, stress-induced translational arrest plays an important role in host antiviral defense. To antagonize this host defense, most viruses have evolved to circumvent SG formation during infection. For example, poliovirus (PV) proteinase 3C cleaves G3BP, leading to effective SG dispersion and virus propagation (6). Influenza A virus nonstructural protein 1 (NS1) has been shown to inactivate PKR and prevent SG formation (7). In the case of human immunodeficiency virus 1 (HIV-1) infection, Staufen1 is recruited in ribonucleoproteins for encapsidation through interaction with the Gag protein to prevent SG formation (8). In contrast, some viruses employ alternative mechanisms of translation initiation and promote SG formation to limit cap-dependent translation of host mRNA (9, 10). In addition, vaccinia virus induces cytoplasmic "factories" in which viral translation, replication, and assembly take place. These factories include G3BP and Caprin-1 to promote transcription of viral mRNA (11).

Japanese encephalitis virus (JEV) belongs to the genus *Flavivirus* within the family *Flaviviridae*, which includes other mosquito-borne human pathogens, such as dengue virus (DENV), West Nile virus (WNV), and yellow fever virus, that frequently cause significant morbidity and mortality in mammals and birds (12). JEV has

Received 15 August 2012 **Accepted** 15 October 2012
Published ahead of print 24 October 2012
Address correspondence to Yoshiharu Matsuura, matsuura@biken.osaka-u.ac.jp.

doi:10.1128/JVI.02186-12

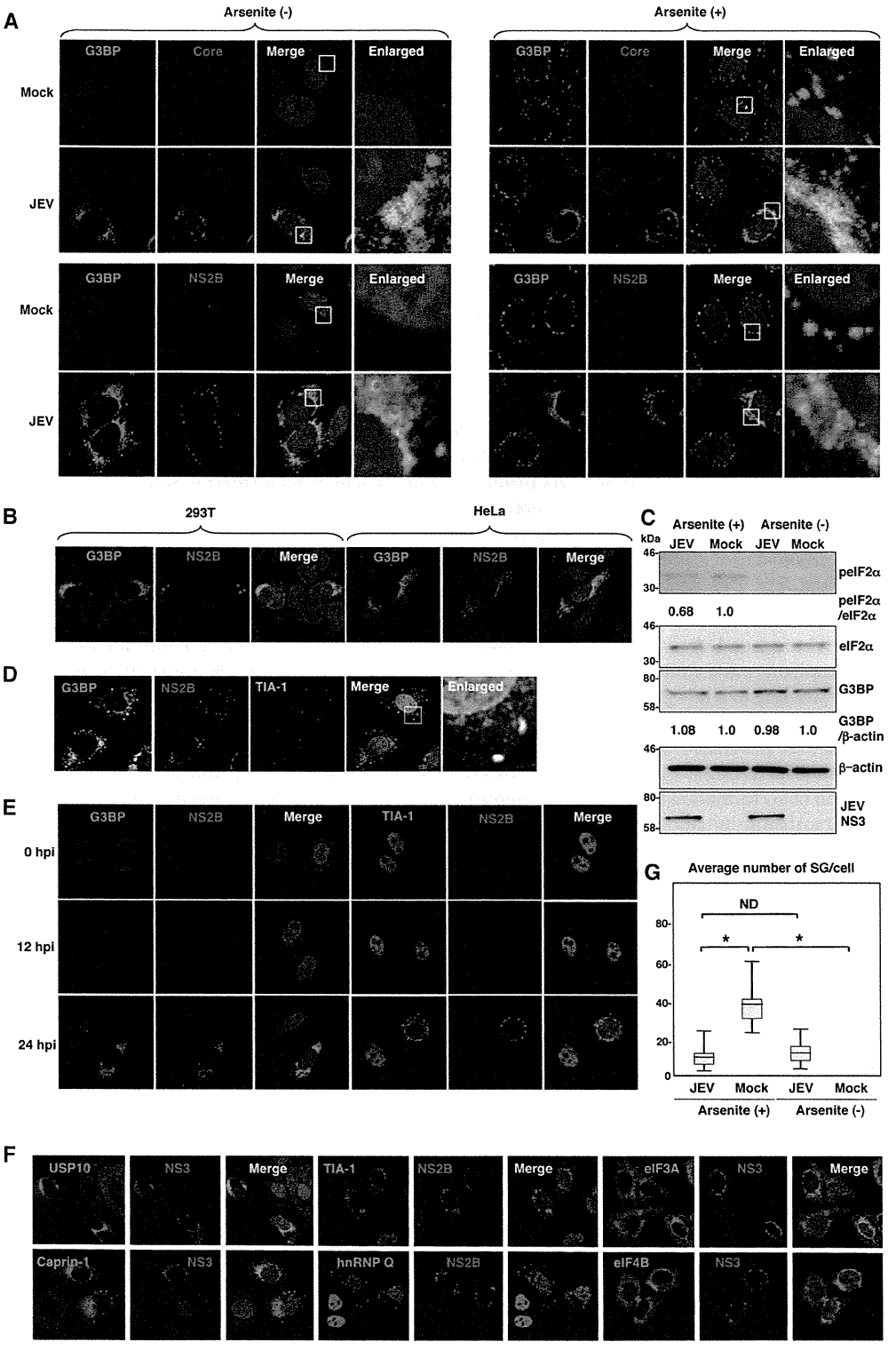

FIG 1 Dynamics of SG-associated factors during JEV infection. (A) Huh7 cells infected with JEV at an MOI of 0.5 were treated with or without 1.0 mM sodium arsenite for 30 min at 37°C, and the levels of expression of G3BP and JEV core protein/NS2B were determined at 24 h postinfection by immunofluorescence analysis with mouse anti-G3BP MAb and rabbit anti-core protein or anti-NS2B PAb, followed by AF488-conjugated anti-mouse IgG (Invitrogen) and AF594-conjugated anti-rabbit IgG, respectively. Cell nuclei were stained with DAPI (blue). (B) Cellular localizations of G3BP and JEV NS2B in 293T and HeLa cells infected with JEV were determined at 24 h postinfection by immunofluorescence analysis with mouse anti-G3BP MAb and rabbit anti-NS2B PAb, followed by AF488-conjugated anti-mouse IgG and AF594-conjugated anti-rabbit IgG, respectively. Cell nuclei were stained with DAPI (blue). (C) Phosphorylation of eIF2α in cells prepared as described in panel A was determined by immunoblotting using the indicated antibodies. The band intensities were quantified by ImageJ

a single-stranded positive-sense RNA genome of approximately 11 kb. The genomic RNA carries a single large open reading frame, and a polyprotein translated from the genome is cleaved co- and posttranslationally by host and viral proteases to yield three structural proteins, the core, precursor membrane (PrM), and envelop (E) proteins, and seven nonstructural (NS) proteins, NS1, NS2A, NS2B, NS3, NS4A, NS4B, and NS5 (13). PrM is further cleaved by the multibasic protease, furin, and matured to membrane (M) protein. The core, M, and E proteins are components of extracellular mature virus particles. NS proteins are not incorporated into particles and are thought to be involved in viral replication, which occurs in close association with ER-derived membranes (14). Previous reports have shown that WNV and DENV inhibit SG formation by sequestering TIA-1 and TIAR through specific interaction with viral RNA (15, 16). In addition, the membrane structure induced by WNV infection was suggested to prevent PKR activation and avoid induction of SG formation (17). In this study, we show that JEV core protein plays an important role in inhibition of SG formation. JEV core protein recruited several SG-associated proteins, including G3BP and USP10, through an interaction with Caprin-1 and suppressed SG formation. Furthermore, a mutant JEV carrying a core protein incapable of binding to Caprin-1 exhibited lower propagation *in vitro* and lower pathogenicity in mice than the wild-type (WT) JEV, suggesting that inhibition of SG formation by the core protein is crucial to antagonize host defense. These results reveal a novel strategy of JEV to inhibit SG formation through an interaction with Caprin-1 and facilitate viral propagation.

MATERIALS AND METHODS

Plasmids. Plasmids encoding FLAG-tagged JEV core protein (pCAGPM-FLAG-Core) and hemagglutinin (HA)-tagged JEV proteins (pCAGPM-HA-JEV proteins) were generated as previously described (18, 19). The cDNA of the core protein of JEV AT31 (amino acid residues 2 to 105) was amplified from the pCAGPM-FLAG-Core plasmid by PCR and cloned into pET21b (Novagen-Merck, Darmstadt, Germany) for expression in bacteria as a His-tagged protein and in pCAG-MCS2-FOS for expression in mammalian cells as a FLAG-One-STrEP (FOS)-tagged protein. The resulting plasmids were designated pET21b-Core-His and pCAG-Core-FOS, respectively. The cDNA of the core protein of DENV2 (amino acid residues 2 to 100) was amplified from the pCAG/FLAG-DEN2C-HA plasmid (19) by PCR and cloned into pCAGPM-N-FLAG. The cDNA of human Caprin-1 was amplified from 293T cells by reverse transcription-PCR (RT-PCR) and cloned into pCAGPM-N-HA (20) and pGEX 6P-1 (GE Healthcare, Buckinghamshire, United Kingdom) for expression in bacteria as a glutathione *S*-transferase (GST) fusion protein and designated pCAGPM-HA-Caprin-1 and pGEX-GST-Caprin-1, respectively. The cDNAs of human G3BP1 and USP10 were also amplified from 293T cells by RT-PCR and cloned into pCAGPM-N-HA. The nucleotide residues of the adenine at 384, adenine at 385, cytosine at 387, and guanine at 388 of the JEV genome in pMWATG1 were replaced with guanine, cytosine, guanine, and cytosine, respectively, by PCR-based mutagenesis to change Lys^{97} and Arg^{98} of the core protein to Ala, yielding pMWAT/KR9798A. The cDNA of the mutant core protein was also cloned into pCAGPM-N-FLAG and pET21b. To generate stable cell lines expressing *Aequorea coerulescens* green fluorescent protein (AcGFP)-fused Caprin-1, the cDNA of human Caprin-1 was amplified by RT-PCR and cloned into pAcGFP N1 (Clontech, Mountain View, CA), and the Caprin-1-AcGFP gene was subcloned into the lentiviral vector pCSII-EF-RfA (21) and designated pCSII-EF-Caprin-1-AcGFP. All plasmids were confirmed by sequencing with an ABI Prism 3130 genetic analyzer (Applied Biosystems, Tokyo, Japan).

Cells and stress treatment. Mammalian cell lines, Vero (African green monkey kidney), 293T (human kidney), Huh7 (human hepatocellular carcinoma), and HeLa (human cervical carcinoma), were maintained in Dulbecco's modified Eagle's minimal essential medium (DMEM) (Sigma, St. Louis, MO) supplemented with 100 U/ml penicillin, 100 mg/ml streptomycin, nonessential amino acids (Sigma), and 10% fetal bovine serum (FBS). The mosquito cell line C6/36 (*Aedes albopictus*) was grown in Leibovitz's L-15 medium with 10% FBS. Huh7 cells were transduced with a lentiviral vector expressing Caprin-1-AcGFP and AcGFP and designated Huh7/Caprin-1-AcGFP and Huh7/AcGFP, respectively. For induction of SGs, cells were treated with sodium arsenite at a final concentration of 1.0 mM in the culture medium for 30 min prior to fixation or lysis of the cells. SG formation was defined morphologically by immunostaining using anti-SG-related factor antibodies described below. Cell viability was determined by using CellTiter-Glo (Promega, Madison, WI) according to the manufacturer's instruction.

Viruses. The wild-type and 9798A mutant of the JEV AT31 strain were generated by the transfection of pMWATG1 and pMWAT/KR9798A, respectively, as described previously (22). Viral infectivity was determined by an immunostaining focus assay as described previously (20), and the results are expressed in focus-forming units (FFU). JEV and DENV serotype 2 New Guinea C strain were amplified in C6/36 cells.

Antibodies. Anti-JEV core rabbit polyclonal antibody (PAb) and anti-JEV NS3 mouse monoclonal antibody (MAb) were prepared as described previously (20, 23). Anti-JEV NS2B rabbit PAb was generated with synthetic peptides of JEV NS2B at Scrum, Inc. (Tokyo, Japan). Anti-DENV core protein rabbit PAb was prepared by using a GST-fused recombinant protein containing amino acid residues 2 to 100 of the DENV core protein. Anti-FLAG mouse MAb (M2) and rabbit PAb and anti-β-actin mouse MAb were purchased from Sigma. Anti-hnRNP Q mouse MAb (ab10687), anti-USP10 rabbit PAb (ab70895), and anti-eIF4B rabbit PAb (ab78916) were purchased from Abcam (Cambridge, United Kingdom). Anti-eIF2α, anti-phospho-eIF2α, and anti-eIF3A rabbit PAbs were purchased from Cell Signaling Technology (Danvers, MA). Anti-HA mouse MAb (HA11), anti-HA rat MAb (3F10), anti-His mouse MAb, anti-GFP mouse MAb (JL-8), anti-JEV envelope protein mouse MAb (6B4A-10), anti-G3BP mouse MAb, anti-TIA-1 goat PAb, anti-Caprin-1 rabbit PAb, and anti-dsRNA mouse MAb were purchased from Covance (Richmond, CA), Roche (Mannheim, Germany), R&D Systems (Minneapolis, MN), Clontech, Chemicon (Temecula, CA), BD Biosciences (Franklin Lakes, NJ), Santa Cruz (Santa Cruz, CA), Proteintech (Chicago, IL), and Bio-

software (NIH, Bethesda, MD), and the relative levels for the indicated proteins are shown based on the level of the mock-infected cells. (D) Cellular localizations of G3BP, NS2B, and TIA-1 in Huh7 cells infected with JEV were determined at 24 h postinfection by immunofluorescence analysis with mouse anti-G3BP MAb, rabbit anti-NS2B PAb, and goat anti-TIA-1 PAb, followed by AF488-conjugated anti-mouse IgG, AF594-conjugated anti-rabbit IgG, and AF633-conjugated anti-goat IgG, respectively. Cell nuclei were stained with DAPI (gray). (E) Dynamics of G3BP and TIA-1 during JEV infection. Huh7 cells infected with JEV were immunostained at 0, 12, and 24 h postinfection (hpi) with mouse anti-G3BP MAb or goat anti-TIA-1 PAb and rabbit anti-NS2B PAb, followed by AF488-conjugated anti-mouse IgG or AF488-conjugated anti-goat IgG and AF594-conjugated anti-rabbit IgG, respectively. Cell nuclei were stained with DAPI (blue). (F) Cellular localization of SG-associated proteins (USP10, Caprin-1, TIA-1, hnRNP Q, eIF3A, and eIF4B) (green, AF488-conjugated secondary antibody) and JEV NS2B/NS3 (red, AF-594-conjugate secondary antibody) in Huh7 cells infected with JEV was determined by immunoblotting at 24 h postinfection. Cell nuclei were stained with DAPI (blue). (G) Numbers of G3BP-positive foci in 30 cells prepared as described in panel A were counted for each experimental condition. Lines, boxes, and error bars indicate the means, 25th to 75th percentiles, and 95th percentiles, respectively. The significance of differences between the means was determined by a Student's *t* test.*, $P < 0.01$; ND, no significant difference.

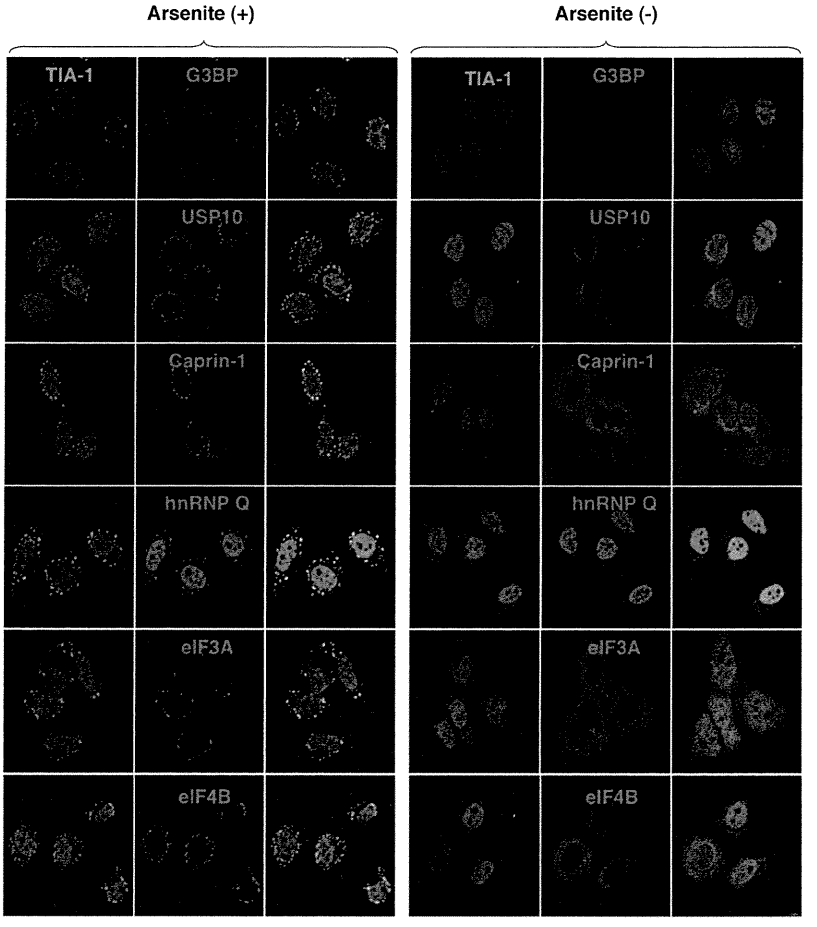

FIG 2 Each SG-associated factor forms SGs under oxidative stress. After treatment with 1.0 mM sodium arsenite for 30 min at 37°C, Huh7 cells were subjected to immunofluorescence analysis with the indicated primary antibodies, followed by AF488-conjugated anti-goat IgG and AF594-conjugated anti-mouse or rabbit IgG. Cell nuclei were stained with DAPI (blue).

center (Szirak, Hungary), respectively. Alexa Fluor (AF)-conjugated secondary antibodies were purchased from Invitrogen (Carlsbad, CA).

Immunofluorescence microscopy. Huh7 cells were fixed in 4% paraformaldehyde in phosphate-buffered saline (PBS) for 15 min at room temperature. After cells were quenched for 10 min with PBS containing 50 mM ammonium chloride (NH_4Cl), they were permeabilized with 0.2% Triton X-100 in PBS for 10 min and blocked with PBS containing 2% bovine serum albumin (BSA) for 30 min at room temperature. The cells were then incubated with the antibodies indicated in the figure legends. Nuclei were stained with 4′,6′-diamidino-2-phenylindole (DAPI). The samples were examined by a Fluoview FV1000 laser scanning confocal microscope (Olympus, Tokyo, Japan).

Transfection, immunoprecipitation, and immunoblotting. Plasmids were transfected into 293T or Huh7 cells by use of TransIT LT1 (Mirus, Madison, WI), and cells collected at 24 h posttransfection were subjected to immunostaining, immunoprecipitation, and/or immunoblotting as described previously (24). The immunoprecipitates were boiled in sodium dodecyl sulfate (SDS) sample buffer and subjected to SDS-polyacrylamide gel electrophoresis (SDS-PAGE). The proteins were transferred to polyvinylidene difluoride membranes (Millipore, Bedford, MA) and incubated with the appropriate antibodies. The immune complexes were visualized with SuperSignal West Femto substrate (Thermo Scientific, Rockford, IL) and detected by use of an LAS-3000 image analyzer system (Fujifilm, Tokyo, Japan).

FOS-tagged purification and mass spectrometry. pCAG-Core-FOS or empty vector was transfected into 293T cells, harvested at 24 h posttransfection, washed with cold PBS, suspended in cell lysis buffer (20 mM Tris-HCl, pH 7.4, 135 mM NaCl, 1% Triton X-100, and protease inhibitor cocktail [Complete; Roche]), and centrifuged at 14,000 × *g* for 20 min at 4°C. The supernatant was pulled down using 50 μl of STrEP-Tactin Sepharose (IBA, Gottingen, Germany) equilibrated with cell lysis buffer for 2 h at 4°C. The affinity beads were washed three times with cell lysis buffer and suspended in 2× SDS-PAGE sample buffer. The proteins were subjected to SDS-PAGE, followed by Coomassie brilliant blue (CBB) staining using CBB Stain One (Nakalai Tesque, Kyoto, Japan). The gels were divided into 10 pieces, and each fraction was trypsinized and subjected to liquid chromatography-tandem mass spectrometry (LC-MS/MS) analysis to identify coimmunoprecipitated proteins. All of the proteins in gels were identified comprehensively, and the proteins detected in cells transfected with pCAG-Core-FOS but not in those with empty vector were regarded as candidates for binding partners of JEV core.

Gene silencing. A commercially available small interfering RNA (siRNA) pool targeting Caprin-1 (siGENOME SMARTpool, human Caprin1) and control nontargeting siRNA were purchased from Dharmacon (Buckinghamshire, United Kingdom) and transfected into 293T cells using Lipofectamine RNAiMAX (Invitrogen) according to the manufacturer's protocol.

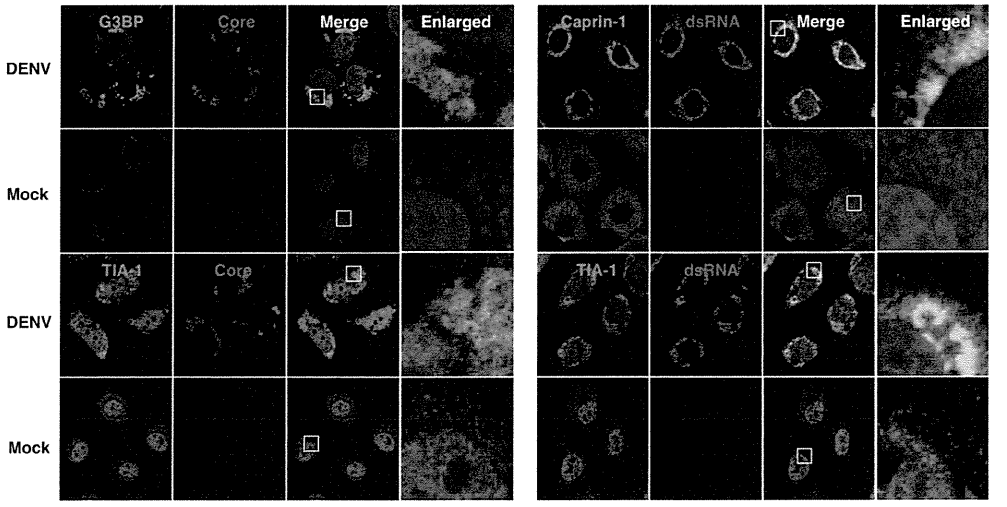

FIG 3 Subcellular localizations of the SG-associated proteins during DENV infection. Cellular localizations of G3BP, Caprin-1, and TIA-1 (green, AF488-conjugated secondary antibody) and viral components (core protein and dsRNA) (red, AF-594-conjugate secondary antibody) in Huh7 cells infected with DENV were determined by immunofluorescence analysis using the appropriate antibodies at 48 h postinfection. Cell nuclei were stained with DAPI (blue).

Preparation of recombinant proteins and GST pulldown assay. His-tagged JEV core protein (core-His) was purified as described in a previous report (25). Briefly, core-His was expressed in *Escherichia coli* (*E. coli*) Rosetta-gami 2(DE3) strain cells (Novagen-Merck) transformed with pET21b-Core-His (WT or 9798A). Bacteria grown to an optical density at 600 nm of 0.6 were induced with 0.5 mM isopropyl-β-D-thiogalactopyranoside (IPTG), incubated for 5 h at 37°C with shaking, collected by centrifugation at 6,000 × *g* for 10 min, lysed in 10 ml of bacteria lysis buffer (50 mM Tris-HCl, pH 7.4, 150 mM NaCl, 1 mM EDTA, 1% Triton X-100, and protease inhibitor cocktail [Complete; Roche]) by sonication on ice, and centrifuged at 10,000 × *g* for 15 min. The supernatant containing core-His was subjected to ammonium sulfate fractionation, followed by cation exchange chromatography with a HiTrap SP column (GE Healthcare). The eluted core-His recombinant protein was dialyzed with 50 mM Tris-HCl buffer containing 150 mM NaCl at 4°C overnight. GST-fused Caprin-1 (GST-Caprin-1) was expressed in *E. coli* BL21(DE3) cells transformed with pGEX-GST-Caprin-1. Bacteria grown to an optical density at 600 nm of 1.0 were induced with 0.1 mM IPTG, incubated for 5 h at 25°C with shaking, collected by centrifugation at 6,000 × *g* for 10 min, lysed in 10 ml of bacteria lysis buffer by sonication on ice, and centrifuged at 10,000 × *g* for 15 min. The supernatant was mixed with 200 μl of glutathione-Sepharose 4B beads (GE Healthcare) equilibrated with bacteria lysis buffer for 1 h at room temperature, and then the beads were washed five times with lysis buffer. Twenty micrograms of GST-Caprin-1 or GST was mixed with equal volumes of the purified core-His for 2 h at 4°C with gentle agitation. The beads were washed five times with bacteria lysis buffer and then suspended in SDS-PAGE sample buffer.

Mouse experiments. Experimental infections were approved by the Committee for Animal Experiment of RIMD, Osaka University (H19-2-0). Female ICR mice (3 weeks old) were purchased from CLEA Japan (Tokyo, Japan) and kept in specific pathogen-free environments. Groups of mice ($n = 10$) were intraperitoneally inoculated with 5×10^4 FFU (100 μl) of the viruses. The mice were observed for 3 weeks after inoculation to determine survival rates. To examine viral growth in the brain, 5×10^4 FFU of the viruses were intraperitoneally administered to the groups of mice ($n = 3$). At 7 days postinfection, mice were euthanized, and the cerebrums were collected. The infectious titers in the homogenates of the cerebrums were determined in Vero cells as described above.

RESULTS

JEV infection confers resistance to SG induction. To examine the formation of SGs in cells infected with JEV, Huh7 cells were infected with JEV at a multiplicity of infection (MOI) of 0.5, and the expression of JEV proteins and an accepted marker for SGs, G3BP, was determined by immunofluorescence analysis at 24 h postinfection. G3BP was mainly accumulated in the perinuclear region and partially colocalized with the JEV core protein, while only partial colocalization with the NS2B protein was also observed (Fig. 1A, left). In addition, a few small G3BP-positive foci were scattered in the cytoplasm. This accumulation of G3BP was observed in not only Huh7 cells but also other cell lines, i.e., 293T and HeLa cells, infected with JEV (Fig. 1B). However, the expression level of G3BP in cells infected with JEV was comparable to that in mock-infected cells (Fig. 1C). To further investigate SG induction by JEV infection, expression of TIA-1, another SG marker, was examined. Although accumulation of TIA-1 in the perinuclear region was not observed, a few TIA-1-positive foci were observed in the JEV-infected cells and were colocalized with G3BP and JEV NS2B, indicating that SG foci were induced in cells infected with JEV (Fig. 1D). The accumulation of G3BP and the aggregation of TIA-1, indicating SG formation, appeared at 24 h postinfection in accord with the expression of viral proteins (Fig. 1E). We further examined the dynamics of other SG-associated factors in cells infected with JEV. Each factor formed clear SGs in cells treated with sodium arsenite, a potent SG inducer eliciting oxidative stress (Fig. 2). As shown in Fig. 1F, three distinct patterns of the subcellular localization of SG components were observed. USP10 and Caprin-1 were accumulated in the perinuclear region and also formed a few small foci scattered throughout the cytoplasm, as seen for G3BP; TIA-1 and hnRNP Q formed cytoplasmic foci but were not accumulated in the perinuclear region; and subcellular localization of eIF3A and eIF4B was not changed. The cytoplasmic foci were confirmed as SGs by immunofluorescence analyses using specific antibodies to SG-associated factors (data not shown). Taken together, these results indicate that JEV infection induces accumulation of several RBPs and formation of a few SGs.

It has been shown previously that infection with WNV or DENV confers resistance to SG formation induced by sodium arsenite (15). To determine the effect of JEV infection on the SG

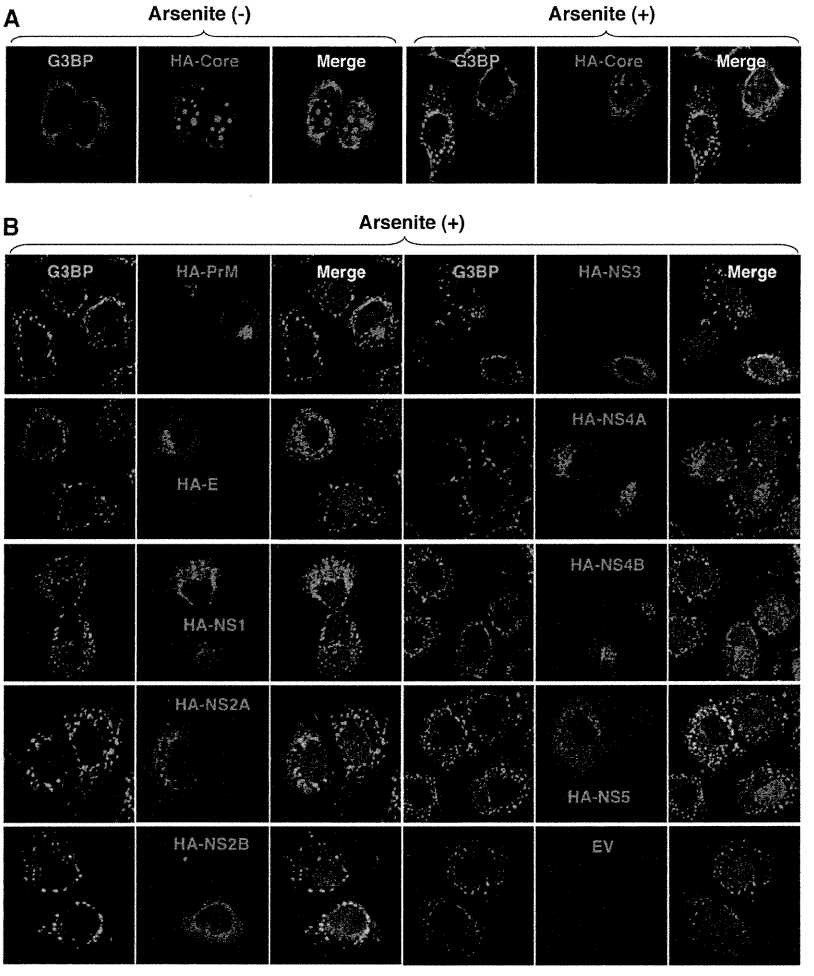

FIG 4 Inhibition of the arsenite-induced SG formation by the expression of JEV proteins. (A) Huh7 cells transfected with a plasmid, pCAGPM-HA-Core, were treated with or without 1.0 mM sodium arsenite for 30 min at 37°C, and the cellular localizations of G3BP and HA-Core were determined at 24 h posttransfection by immunofluorescence analysis with mouse anti-G3BP MAb and rat anti-HA MAb, followed by AF488-conjugated anti-mouse IgG and AF594-conjugated anti-rat IgG, respectively. Cell nuclei were stained with DAPI (blue). (B) Huh7 cells, which were separately transfected with a plasmid expressing an individual viral protein (pCAGPM-HA-JEV protein) as indicated in the figure, were treated with 1.0 mM sodium arsenite for 30 min at 37°C and subjected to an immunofluorescence assay using mouse anti-G3BP MAb and rat anti-HA MAb, followed by AF488-conjugated anti-mouse IgG and AF594-conjugated anti-rat IgG, respectively. Cell nuclei were stained with DAPI (blue).

formation induced by sodium arsenite, JEV-infected cells were treated with 0.5 mM sodium arsenite for 30 min at 24 h postinfection. Although many G3BP-positive foci were observed in mock-infected cells by the treatment with sodium arsenite, accumulation of G3BP in the perinuclear region was observed in the JEV-infected cells (Fig. 1A, right), and the numbers of G3BP-positive foci in the JEV-infected cells were less than those in the mock-infected cells (Fig. 1G). Although it has been reported that a significant reduction of the phosphorylation at Ser^{51} of eIF2α in cells treated with arsenite was induced by infection with WNV (15), the phosphorylation of eIF2α was slightly suppressed in the JEV-infected cells (Fig. 1C). Furthermore, while previous studies reported that Caprin-1 and TIA-1 were colocalized with dsRNA in cells infected with DENV (15, 26), no colocalization of G3BP or TIA-1 with the DENV core protein was observed in the present study (Fig. 3), suggesting that the mechanisms of the viral circumvention of SG formation in cells infected with JEV are different from those in cells infected with WNV and DENV.

JEV core protein suppresses SG formation induced by sodium arsenite. To elucidate the molecular mechanisms of suppression of SG formation induced by sodium arsenite during JEV infection, we tried to identify which viral protein(s) is responsible for the SG inhibition. Since G3BP was colocalized with JEV core protein, we first examined the involvement of the core protein in the perinuclear accumulation of G3BP and in the suppression of SG formation. The expression of JEV core protein alone induced the accumulation of G3BP in the perinuclear region (Fig. 4A, left panel) and suppressed sodium arsenite-induced SG formation (Fig. 4A, upper right cell in the right panel), similarly to JEV infection. In contrast, inhibition of SG formation induced by sodium arsenite was not observed in cells expressing other JEV proteins (Fig. 4B). These results suggest that JEV core protein is responsible for the circumvention of the SG formation observed in cells infected with JEV.

JEV core protein directly interacts with Caprin-1, an SG-associated cellular factor. Since JEV core protein was suggested to

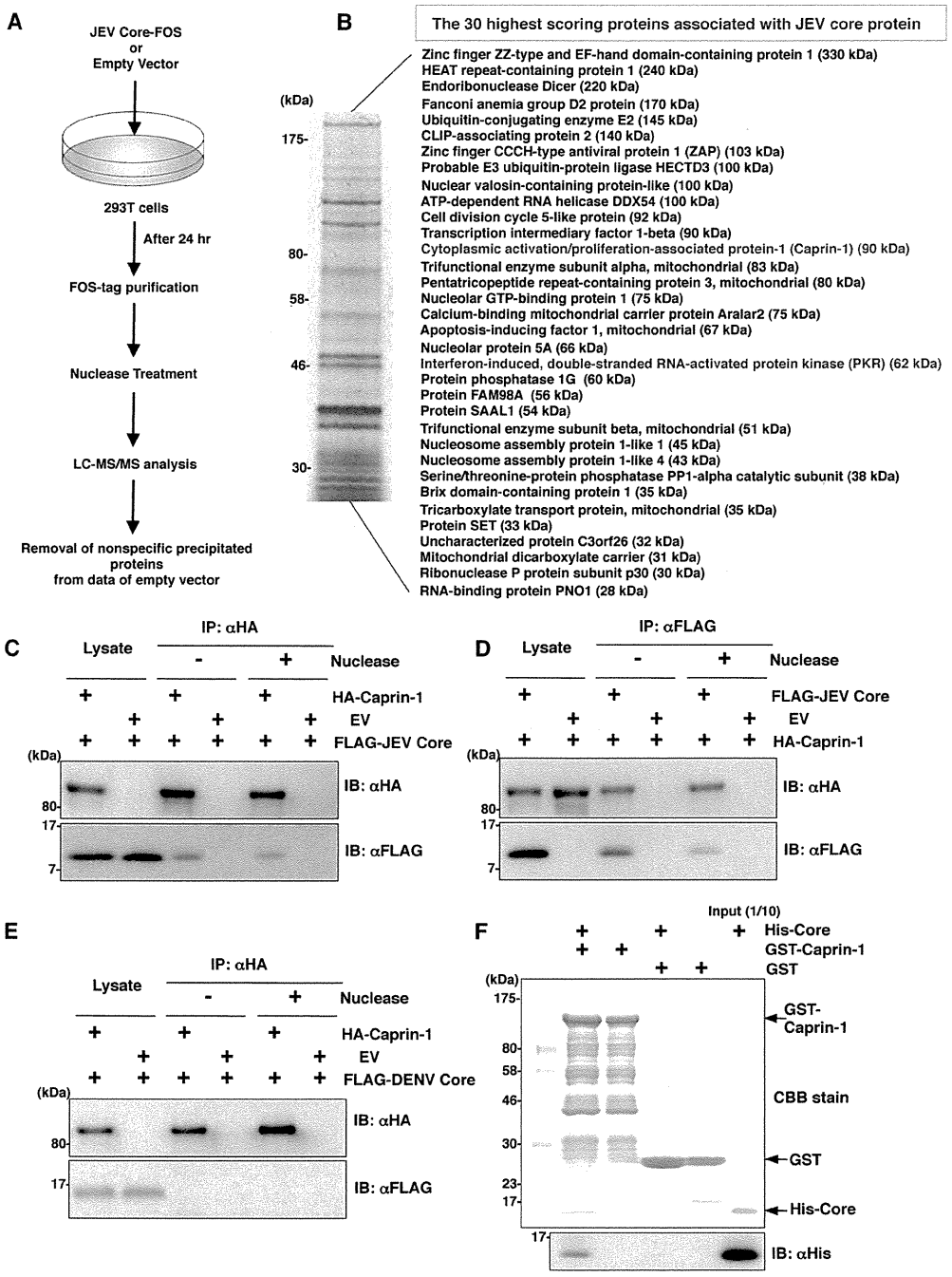

FIG 5 JEV core protein directly interacts with Caprin-1, an SG-associated cellular factor. (A) Identification of host cellular proteins associated with JEV core protein by FOS-tagged purification and LC-MS/MS analysis. Overview of the FOS-tagged purification of cellular proteins associated with JEV core protein. (B) The 30 candidate proteins as binding partners of JEV core protein exhibiting high scores are listed. PKR and Caprin-1 are indicated in red. (C and D) FLAG-JEV core protein and HA-Caprin-1 were coexpressed in 293T cells, and the cell lysates harvested at 24 h posttransfection were treated with or without micrococcal nuclease for 30 min at 37°C and immunoprecipitated (IP) with anti-HA (αHA) or anti-FLAG (αFLAG) antibody, as indicated. The precipitates were subjected to immunoblotting (IB) to detect coprecipitated counterparts. (E) FLAG-DENV core protein was coexpressed with HA-Caprin-1 in 293T cells, immunoprecipitated with anti-HA antibody, and immunoblotted with anti-HA or anti-FLAG antibody. (F) His-tagged JEV core protein was incubated with either GST-fused Caprin-1 or GST for 2 h at 4°C, and the precipitates obtained by GST pulldown assay were subjected to CBB staining and immunoblotting with anti-His antibody.

participate in the inhibition of SG formation, we tried to identify cellular factors associated with the core protein by LC-MS/MS analysis, as shown in Fig. 5A. Among the 30 factors with the best scores, two SG-associated proteins, PKR (Mascot search score, 206) and Caprin-1 (Mascot search score, 153), were identified as binding partners of JEV core protein (Fig. 5B). Although PABP1, hnRNP Q, Staufen, G3BP, and eIF4G were also identified, their scores were lower than those of PKR and Caprin-1. Because the

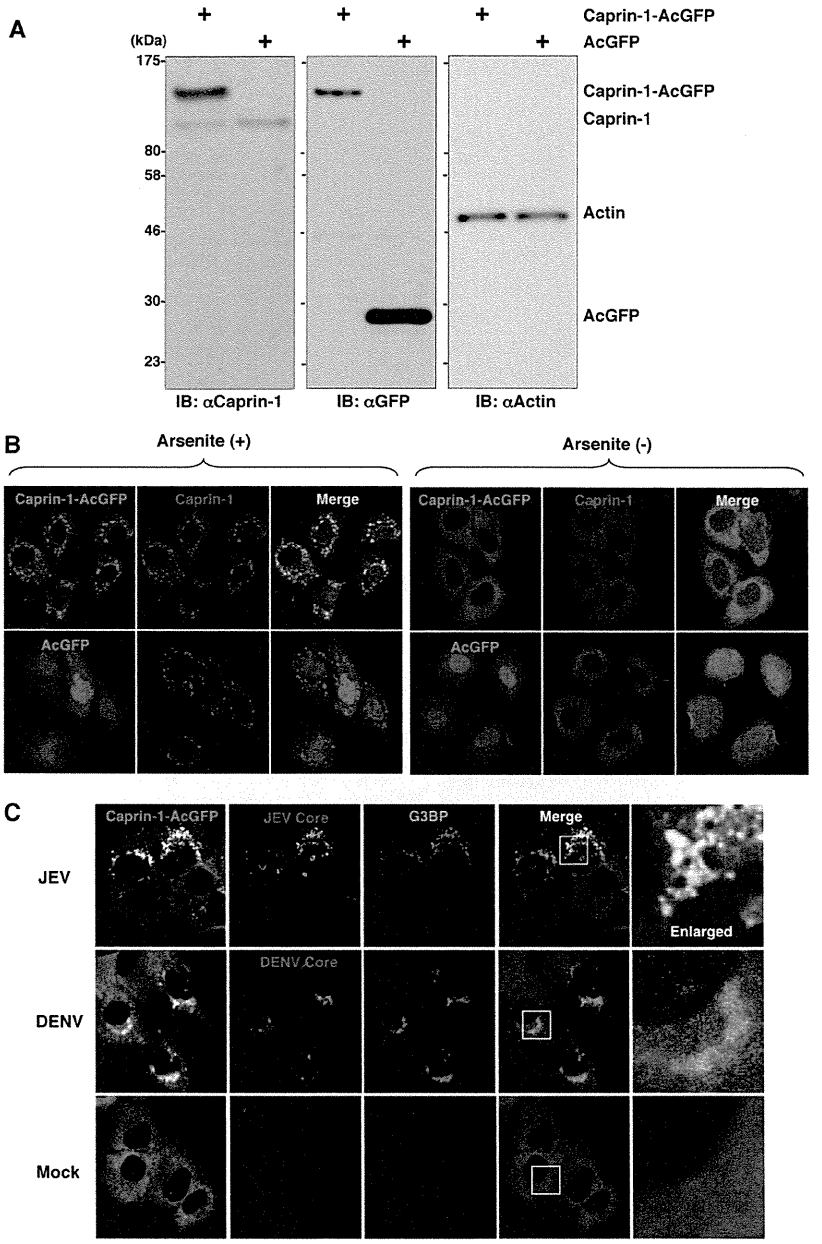

FIG 6 Caprin-1 is colocalized with the JEV core protein in the perinuclear region. (A) Expression of Caprin-1 fused with AcGFP (Caprin-1-AcGFP), Caprin-1, actin, or AcGFP in lentivirally transduced Huh7 cells was determined by immunoblotting using the appropriate antibodies. (B) Subcellular localization of Caprin-1-AcGFP or AcGFP (green) and endogenous Caprin-1 (red) in cells treated with/without 1.0 mM sodium arsenite for 30 min at 37°C was determined by immunofluorescence assay with rabbit anti-Caprin-1 PAb and AF594-conjugated anti-rabbit IgG. Cell nuclei were stained with DAPI (blue). (C) Huh7/Caprin-1-AcGFP cells were infected with either JEV or DENV at an MOI of 0.5, and the cellular localizations of JEV and DENV core (red) with Caprin-1-AcGFP and G3BP (blue) were determined at 24 h and 48 h postinfection, respectively. Cells were stained with mouse anti-G3BP MAb and rabbit anti-JEV or DENV core protein PAb, followed by AF633-conjugated anti-mouse IgG and AF594-conjugated anti-rabbit IgG, respectively, and examined by immunofluorescence analysis.

results shown in Fig. 1B suggest that the inhibition of SG formation takes place downstream of eIF2α phosphorylation, we focused on Caprin-1 as a key factor involved in the inhibition of SG formation in cells infected with JEV. To confirm the specific interaction of JEV core protein with Caprin-1, FLAG-JEV core protein and HA-Caprin-1 were coexpressed and immunoprecipitated with anti-HA or anti-FLAG antibody in the presence or absence of nuclease. FLAG-JEV core protein was coprecipitated with HA-Caprin-1 irrespective of nuclease treatment (Fig. 5C and D), suggesting that the interaction between JEV core protein and Caprin-1 is a protein-protein interaction. On the other hand, FLAG-DENV core protein was not coprecipitated with HA-Caprin-1 (Fig. 5E), indicating that the interaction with Caprin-1 was specific for JEV core protein. Next, the direct interaction be-

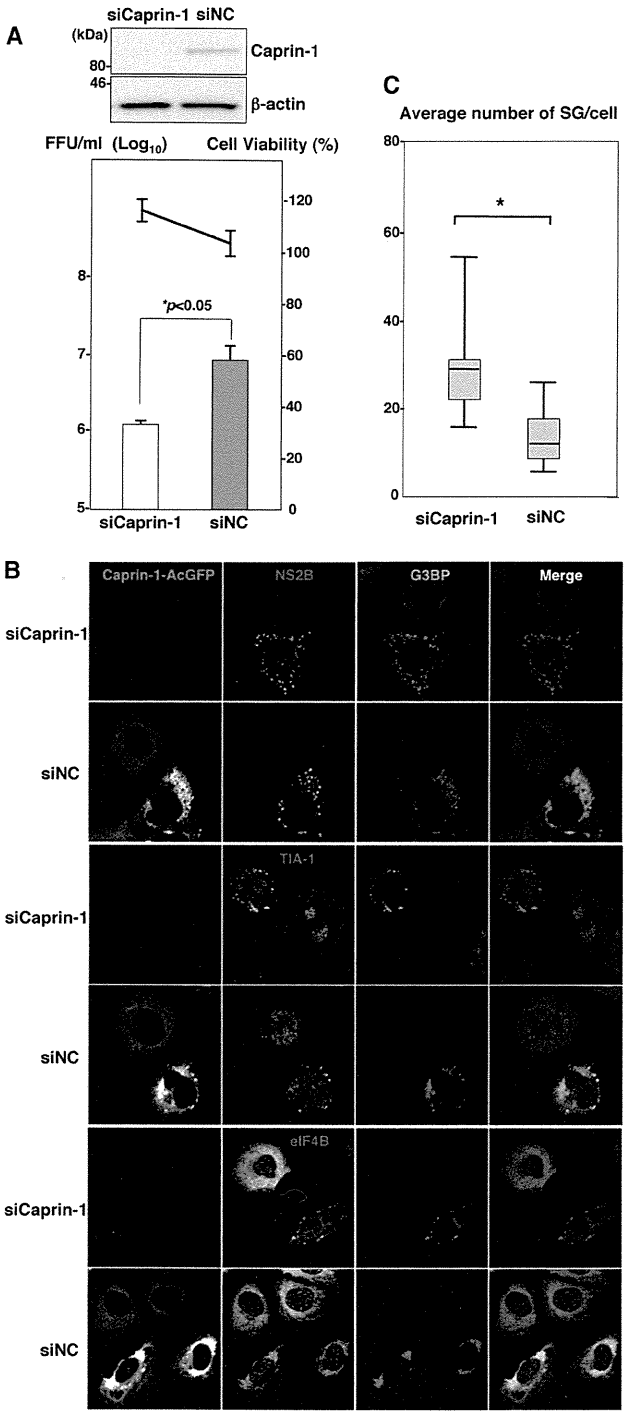

FIG 7 Knockdown of Caprin-1 cancels SG inhibition during JEV infection and suppresses viral propagation. (A) (Upper) The levels of expression of Caprin-1 in cells transfected with either siCaprin-1 or siNC was determined by immunoblotting using anti-Caprin-1 and anti-β-actin antibodies at 72 h posttransfection (top panel). At 48 h posttransfection with either siCaprin-1 or siNC, Huh7/Caprin-1-AcGFP cells were inoculated with JEV at an MOI of 0.5. At 24 h postinfection (72 h posttransfection), the infectious titers in the supernatants were determined by focus-forming assay in Vero cells (bottom panel, bar graph). Cell viability was determined at 72 h posttransfection and calculated as a percentage of the viability of cells treated with siNC (bottom panel, line graph). The results shown are from three independent assays, with the error bars representing the standard deviations. (B) At 48 h posttransfection with either siCaprin-1 or siNC, Huh7/Caprin-1-AcGFP cells were inoculated with JEV at an MOI of 0.5. The cellular localizations of SG-associated factors and JEV NS2B were determined at 24 h postinfection (72 h posttransfection) by immunofluorescence analysis with mouse anti-G3BP MAb and rabbit anti-NS2B PAb, rabbit anti-eIF4B PAb, or goat anti-TIA-1 PAb, followed by AF633-conjugated anti-mouse IgG and AF594-conjugated anti-rabbit IgG or AF594-conjugated anti-goat IgG, respectively. (C) Numbers of G3BP-positive foci in 30 cells prepared as described in panel B were counted. Lines, boxes, and error bars indicate the means, 25th to 75th percentiles, and 95th percentiles, respectively. The significance of differences between the means was determined by a Student's *t* test. *, $P < 0.01$.

tween JEV core protein and Caprin-1 was examined by a GST-pulldown assay using purified proteins expressed in bacteria. The His-tagged core protein was coprecipitated with GST-tagged Caprin-1, suggesting that JEV core protein directly interacts with Caprin-1 (Fig. 5F).

To further determine the cellular localization of Caprin-1 in JEV-infected cells, Caprin-1 fused with AcGFP (Caprin-1-AcGFP) was lentivirally expressed in Huh7 cells. The levels of expression and recruitment of Caprin-1-AcGFP into SGs were determined by immunoblotting and immunofluorescence analysis, respectively (Fig. 6A and B). In cells infected with JEV, Caprin-1-AcGFP was concentrated in the perinuclear region and colocalized with core protein and G3BP, while no colocalization of the proteins was observed in cells infected with DENV (Fig. 6C), suggesting that Caprin-1 directly interacts with JEV core protein in the perinuclear region of the infected cells.

Knockdown of Caprin-1 cancels SG inhibition during JEV infection and suppresses viral propagation. To assess the biological significance of the interaction of JEV core protein with Caprin-1 in JEV propagation, the expression of Caprin-1 was suppressed by using Caprin-1-specific siRNAs (siCaprin-1). Transfection of siCaprin-1 efficiently and specifically knocked down the expression of Caprin-1 with a slight increase of cell viability and decreased the production of infectious particles in the culture supernatants of cells infected with JEV, in comparison with those treated with a control siRNA (siNC) (Fig. 7A). Furthermore, immunofluorescence analyses revealed that knockdown of Caprin-1 increased the number of G3BP-positive granules colocalized with SG-associated factors, including TIA-1 and eIF4B, and inhibited the G3BP concentration in the perinuclear region (Fig. 7B and C). These results suggest that knockdown of Caprin-1 suppresses JEV propagation through the induction of SG formation.

Lys^{97} and Arg^{98} in the JEV core protein are crucial residues for the interaction with Caprin-1. To determine amino acid residues of the core protein that are required for the interaction with Caprin-1, we constructed a putative model based on the structural information of the DENV core protein previously resolved by nuclear magnetic resonance (NMR) (27), as shown in Fig. 8A. Based on this model, we selected hydrophobic amino acids, which were located on the solvent-exposed side in the α1 and α4 helices, as amino acid residues responsible for the binding to host proteins. Amino acid substitutions in each of the α-helices shown in Fig. 8B were designed in the context of FLAG-Core (Mα1 and Mα4), and the interaction of FLAG-Core mutants with Caprin-1 was examined by immunoprecipitation analysis. WT and Mα1, but not Mα4, core proteins were immunoprecipitated with Caprin-1 (Fig. 8B). To determine the amino acids responsible for interaction with Caprin-1, further alanine substitutions were introduced in the α4 helix, and the interaction was examined by immunopre-